

Review

# Cosmic-Ray Acceleration and Magnetic Fields in Galaxy Clusters and Beyond: Insights from Radio Observations

Denis Wittor <sup>1,2</sup><sup>1</sup> Hamburger Sternwarte, Gojenbergsweg 112, 21029 Hamburg, Germany; dwittor@hs.uni-hamburg.de<sup>2</sup> Dipartimento di Fisica e Astronomia, Università di Bologna, Via Gobetti 93/2, 40122 Bologna, Italy

**Abstract:** The discovery of diffuse radio emission in galaxy clusters proved the existence of energetic cosmic-ray electrons and cosmic magnetic fields on Mpc-scales in the Universe. Furthermore, both magnetic fields and cosmic-ray electrons are predicted to exist beyond galaxy clusters, namely, in the filaments and voids of the cosmic web. Recent detection of diffuse radio emission in intercluster bridges—the region between two merging clusters—strengthens the theory that both cosmic magnetic fields and cosmic-ray electrons exist on these large scales. Radio observations are our most powerful tool to study cosmic magnetic fields and cosmic-ray electrons in the Universe. The recent improvements in radio astronomy, including the exploration of the low-frequency radio sky, have led to the discovery of countless new radio sources, and hence a new understanding of the origin and evolution of cosmic magnetic fields and cosmic-ray electrons. In this contribution, we summarise the newest discoveries in the field. Furthermore, we discuss what these new radio observations teach us about cosmic magnetic fields and cosmic rays in galaxy clusters and beyond.

**Keywords:** cosmic-rays; magnetic fields; galaxy clusters; cosmic web; radio emission

## 1. Introduction

Magnetic fields are indispensable in the Universe. They exist on all scales ranging from planets to galaxies all the way to the cosmic web (e.g., [1] and references therein). The cosmic web is the web-like structure that determines the shape of the Universe on Mpc-scales and beyond: gaseous filaments permeate the space, and they are separated by underdense regions called voids (for details, we point to the review “The connection between galaxy clusters and the large scale structures of the cosmic web” of this Special Issue). The intersections of the filaments are inhabited by galaxy clusters: large assemblies of mass that consist of dark matter, galaxies, and the intracluster medium (ICM). The ICM is a hot and dilute plasma that fills the space inbetween the galaxies (e.g., [2–4]).

Large-scale magnetic fields are expected to exist in the different components of the cosmic web (e.g., [5,6]). While observations have proven the existence of  $\mu\text{G}$  magnetic fields in galaxy clusters, they have yet to be directly observed in the cosmic filaments and voids. Currently, only limits of a few nG exist for the magnetic fields in filaments (e.g., [7] and references therein). The limits on the magnetic fields in voids are even lower and they range between  $10^{-16}$  G to  $10^{-10}$  G (e.g., [7]). Recently, magnetic fields of a few  $0.1 \mu\text{G}$  have been detected in intercluster bridges, the regions between two merging clusters [8]. In all cases, the plasma  $\beta$ —the ratio of thermal pressure to magnetic pressure—is predicted to be large, i.e.,  $\beta \approx 100$ .

The true origin of cosmic magnetic fields is still unknown and two scenarios have been proposed (e.g., [9] and references therein): in the *primordial* scenario, magnetic fields are generated in the early Universe. In the *astrophysical* scenario, magnetic fields are produced on galactic scales and are then transported to larger scales. While the reality might be a combination of both scenarios, understanding the true origin of magnetic fields is still one of the “holy grails” in modern astrophysics.



**Citation:** Wittor, D. Cosmic-Ray Acceleration and Magnetic Fields in Galaxy Clusters and Beyond: Insights from Radio Observations. *Universe* **2023**, *9*, 319. <https://doi.org/10.3390/universe9070319>

Academic Editor: Lorenzo Iorio

Received: 19 March 2023

Revised: 22 June 2023

Accepted: 27 June 2023

Published: 3 July 2023



**Copyright:** © 2023 by the author. Licensee MDPI, Basel, Switzerland. This article is an open access article distributed under the terms and conditions of the Creative Commons Attribution (CC BY) license (<https://creativecommons.org/licenses/by/4.0/>).

The magnetic fields in galaxy clusters are well studied. Here, large-scale diffuse radio emission traces the cluster magnetic fields. Moreover, the Faraday rotation of polarised background sources can be used to indirectly study the cluster magnetic fields (e.g., [10–15]). Unfortunately, these observations do not provide any information on the origin of the cosmic magnetic fields, as dynamo action and turbulence have erased any footprints of potential primordial fields. On the other hand, the footprints of primordial magnetic fields, if they exist, should be visible in the filaments and voids of the cosmic web [7,16,17].

In galaxy clusters, the diffuse radio emission is synchrotron emission, that is produced by cosmic-ray electrons<sup>1</sup> gyrating around the magnetic fields. Historically, the sources of diffuse radio emission have been classified as giant radio halos, mini-radio halos, and radio relics. Moreover, with the advent of low-frequency radio observations, we have started to detect fossil plasma sources, radio phoenixes, and other steep-spectrum sources (see [11,13,18] for recent reviews). As an example, Figure 1 displays the diffuse radio emission observed in the galaxy cluster Abell 2744 [19].

While halos, mini-halos, and relics are produced by different mechanisms, they have one important thing in common: they must be produced by cosmic-ray electrons that have been accelerated in situ in the ICM, and their emission cannot be related to any individual cluster galaxies. For all sources, the corresponding argument is similar. Typically, these diffuse radio sources are large, i.e., 1–2 Mpc in the cases of halos and relics, and 0.2–0.5 Mpc in the case of mini-halos. The timescales required by a single source to cover such large volumes, i.e., on the order of Gyr, is significantly larger than the possible age of the cosmic-ray electrons, i.e., 10s to 100s of Myr. Hence, the cosmic-ray electrons cannot live long enough to diffuse across the required volume and, therefore, they can only be produced in situ in the ICM [20].

It is commonly accepted that radio relics are produced by the shock acceleration of cosmic-ray electrons [21]. On the other hand, giant radio halos are expected to be produced by turbulent re-acceleration of cosmic-ray electrons [22,23]. The origin of radio mini-halos is less certain. They could be either produced by turbulent re-acceleration, as well, or by hadronic collisions between cosmic-ray protons and the thermal ICM protons [24].

Both in cosmic filaments and cosmic voids, magnetic field amplification is expected to be inefficient (e.g., [6] and references therein). Hence, the magnetic fields are predicted to be weak, and the corresponding radio emission is below the limits of current radio instruments. Therefore, no direct measurements of magnetic fields in cosmic filaments and cosmic voids exists. Fortunately, Faraday rotation measurements of background radio galaxies are used to indirectly constrain the magnetic fields in cosmic filaments and cosmic voids. The observations provide upper limits on the field strengths [25–28]. Recently, there have been attempts to study the magnetic fields in filaments by stacking radio observations [29,30].

This review focuses on the presentation of the newest insights about magnetic fields and cosmic-ray acceleration in galaxy clusters and beyond. As said above, different types of diffuse radio sources provide the best information about the cluster magnetic fields. These radio sources are produced by cosmic-ray electrons that are accelerated in situ in the ICM. However, in most cases the magnetic fields play a crucial role in the acceleration processes themselves and, hence, magnetic fields and cosmic-ray acceleration cannot be studied independently.

The study of magnetic fields and cosmic-ray acceleration in the largest structures of the Universe is a fast evolving field. Especially, the increasing number of new radio facilities, the improving instrumentation and algorithms to reduce the data, as well as the exploration of the low-frequency radio sky are responsible for huge and fast scientific advances in the field<sup>2</sup>. To summarise all these works in a single review is an almost impossible task. Hence, this review is meant to give a broad overview on the recent advances in the field, and to encourage the interested reader to search the literature.

This review is structured as follows: in Section 2, we discuss how galaxy clusters form and how different gas motions are driven in the ICM. These large-scale motions are relevant for both cosmic-ray acceleration and magnetic field amplification. In Section 3, we discuss

the different observational methods used to study magnetic fields and, hence, cosmic rays. In the following section, Section 4, we summarise how magnetic fields evolve over cosmic time. Thereafter, we will present the different radio sources in galaxy clusters, including the underlying particle acceleration mechanism and how they provide information about the magnetic fields. In Section 5 and Section 6, we discuss the physics of radio halos and radio relics. In Section 7, we present the new type of radio sources that have been discovered in recent years. We will briefly discuss the magnetic fields and cosmic-ray acceleration mechanism beyond clusters in Section 8. Finally, we conclude this work in Section 9.

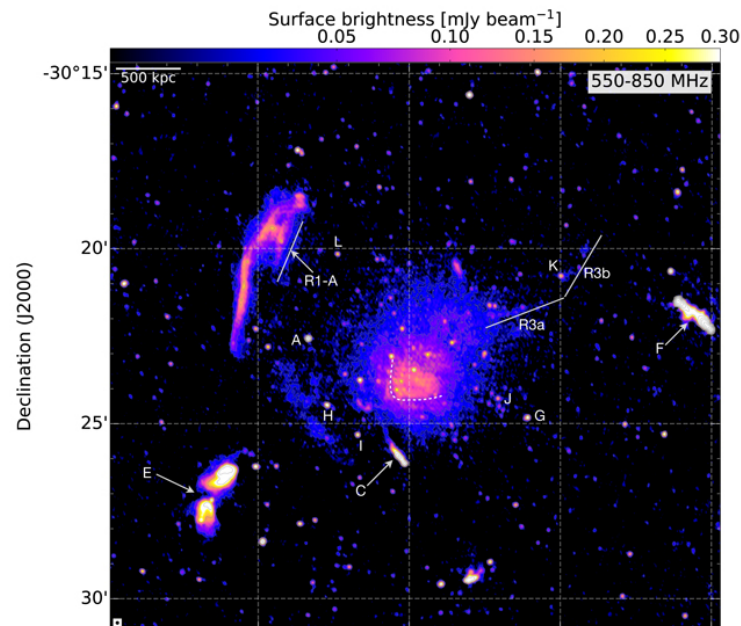


**Figure 1.** Example of diffuse emission in a galaxy cluster taken from Rajpurohit et al. [19]. The figure shows the galaxy cluster Abell 2774 observed at 550–850 MHz. The source R1 is a radio relic, located at the cluster periphery. The central radio emission is a radio halo. The emission labelled as R3 is also expected to be relic-like emission. The remaining sources are either radio galaxies or background sources. Reproduced with permission from Rajpurohit et al.; published by A&A 2021.

## 2. Large-Scale Motions in the ICM

Before the discussion of the origin and evolution of magnetic fields, it is necessary to introduce some of the large-scale motions that are present in the ICM. These gas motions are, namely, turbulence, shock waves, and cold fronts [31–35]. All three of them are driven naturally in the ICM and they play crucial roles in the acceleration of cosmic rays. As each of these would deserve its own review, we briefly summarise their main properties in the following and point to the literature for more elaborated discussions.

Both simulations and observations have shown the presence of turbulent motions in the ICM, with Reynolds numbers of  $Re \geq 1000$  (e.g., [36–41]). These turbulent motions are dominantly solenoidal (divergence-free) but compressive (curl-free) turbulence can also be present [42,43]. On the large cluster scales, i.e., Mpc-scales, turbulence is driven by cluster mergers and the accretion of matter (e.g., [44,45]). On the smaller galactic scales, i.e., tens of kpc-scales, AGN, galactic motions, and magneto-thermal instabilities are the drivers of turbulence (e.g., [46–48]). ICM turbulence is predicted to be Kolmogorov like, i.e., with an energy spectrum of  $E(k) \propto k^{-5/3}$  [49], with turbulent velocities of the order of  $\sim 100$ – $1000$  km/s. In fact, the Hitomi satellite measured a velocity dispersion of  $164 \pm 10$  km/s in the central region of the Perseus cluster [50].

Collisionless shock waves are naturally produced in the ICM by cluster mergers and the accretion of matter (e.g., [37]). There is a whole “zoo” of shock waves that are driven during the processes of structure formation: internal and external shocks, merger

shocks, run away shocks, equatorial shocks, etc. (e.g., [51–55] and references therein). Independently of their classification, most of these shocks are found or are predicted to be in the low Mach number regime—i.e., Mach numbers of a few. Only, external shocks, that occur in the cluster outskirts where the cold gas from voids is accreted onto the cluster, are expected to have Mach numbers of the order of a hundred [33]. However, external shocks are energetically unimportant, as they only exist in low-density regions, where they process low energy fluxes [56]. Hence, mostly internal shocks and merger shocks are relevant for the heating of the ICM.

Cold fronts are contact discontinuities that are similar to shock waves [37,57]. However, the main difference is that the density jump and temperature jump point into opposite directions, i.e., the denser side of the discontinuity is the colder one. Cold fronts are expected to be produced by subsonic gas motions that are driven by cluster mergers and accretion. Cold fronts can be further sub-divided into *remnant-cores*, *sloshing*, and *streams*. However, this sub-classification is not relevant for this review and we point the interested reader to the literature (e.g., [6,58,59] and references therein).

### 3. Measuring Magnetic Fields and Cosmic Rays

There are several ways to obtain information about the magnetic fields and cosmic rays in the ICM. Several review papers have explained these in great detail [11,13,18]. In the following, we present the key points and we point to the literature for specific details.

In galaxy clusters, diffuse radio emission—in the form of radio relics, radio halos and mini-halos—is our best tracer of cosmic magnetic fields and cosmic rays (see [11,18] for recent reviews). This diffuse emission is synchrotron radiation, and, hence, it is directly produced by cosmic rays spiralling around the magnetic fields (e.g., see [60] for the physics of synchrotron radiation). In the optically thin case, the total synchrotron emission depends on the magnetic field strength, the energy distribution of the cosmic-ray electrons, and the pitch angle, i.e., the angle between the magnetic field and electron velocity. Hence, the cosmic-ray electron distribution must be known to derive the magnetic field strength from the synchrotron emission. Before discussing such methods, it is necessary to present some of the standard assumptions about cosmic-ray electrons.

It is commonly assumed that the different cosmic-ray populations in the ICM are described by a power-law distribution in energy (e.g., [18]):

$$n_{\text{CRE}}(E) \propto E^{-\delta}. \quad (1)$$

The spectral index of the energy distribution  $\delta$  is directly connected to the observed radio spectral index  $\alpha$ :

$$\alpha = \frac{\delta - 1}{2}, \quad (2)$$

implying that the radio spectrum is in the form

$$F(\nu) \propto \nu^{-\alpha}. \quad (3)$$

For the diffuse radio sources in galaxy clusters, the radio spectrum is mostly steep, i.e.,  $\alpha \lesssim -1$ . As we will discuss below, the specific value of the radio spectral index  $\alpha$  depends on the acceleration and ageing processes. From Equation (3), it follows that the diffuse radio emission is brighter at low observing frequencies than at high observing frequencies. Consequently, low-frequency observations are favoured to detect diffuse radio emission, produced by a cosmic-ray population with a steep energy distribution. Moreover, aged cosmic rays are still visible at MHz frequencies while they are already below the detection limits of most current facilities at GHz frequencies.

As stated above, the cosmic-ray distribution must be known to translate the diffuse radio emission into any information on the magnetic field. Vice versa, the magnetic field

must be known to derive the cosmic-ray distribution. However, normally neither of the two is well constrained, causing a degeneracy. Hence, additional assumptions are required.

One “method” to break the degeneracy of magnetic fields and cosmic rays is the “method” of *energy equipartition* [61]. Here, it is assumed that within the radio source, the total energy density of the relativistic plasma—the energy stored in the cosmic rays and in the magnetic fields—is at its minimum. This minimum energy is reached when the energies stored in magnetic fields and in cosmic rays are approximately equal—they are in equipartition. These assumptions allow the magnetic field of equipartition to be derived (e.g., [61] and references therein):

$$B_{\text{eq}} \approx 1.1 \gamma_{\text{min}}^{\frac{1-2\alpha}{3+\alpha}} \left( \frac{L_{\nu}(1 + K_{e/p})}{\Phi V} \right)^{\frac{1}{3+\alpha}} \tag{4}$$

Here,  $L_{\nu}$  is the observed synchrotron luminosity,  $K_{e/p}$  is the ratio of energy stored in electrons and protons,  $\alpha$  is the spectral index,  $\gamma_{\text{min}}$  is the Lorentz factor, and  $\Phi$  is the fraction of the volume  $V$  that is occupied by magnetic fields and cosmic rays. However, the energy equipartition method is inherently uncertain, as several assumptions are required a priori. These include assumptions about the volume fraction occupied by both the cosmic rays and the magnetic fields, about the ratio between the energy stored in electrons and heavier ions, or about the shape of the cosmic-ray electron population.

Additional limits on the magnetic field come from the non-detection of inverse Compton emission (e.g., [62]). In principle, the cosmic rays that produce the diffuse radio emission in clusters should also produce inverse Compton emission that is independent of the magnetic field. A detection of both the inverse Compton emission and the diffuse radio emission will give deep constraints on the magnetic field strengths. However, such an inverse Compton signal has never been confirmed. Only recently, Mirakhor et al. [63] discovered potential signs of this non-thermal X-ray emission in the cluster SPT-CL J2031-4037. Nevertheless, the non-detection of inverse Compton emission puts a lower limit on the magnetic field strength, if correlated with the observed radio emission (e.g., [61] and references therein):

$$B_{\text{IC}} = \left( \frac{f_{\text{radio}}(\nu_{\text{radio}})}{f_{\text{X-ray}}(\nu_{\text{X-ray}})} \right)^{\frac{2}{\delta+1}} \left( \frac{\nu_{\text{radio}}}{\nu_{\text{X-ray}}} \right)^{\frac{\delta-1}{\delta+1}} \tag{5}$$

Here,  $f_{\text{radio}}$  and  $f_{\text{X-ray}}$  are the radio flux at frequency  $\nu_{\text{radio}}$  and X-ray flux at frequency  $\nu_{\text{X-ray}}$ , respectively.  $\delta$  is the spectral index of the cosmic-ray electron distribution.

In a similar manner,  $\gamma$ -ray emission can be used to constrain the cluster magnetic fields. If the diffuse radio emission in the ICM is of pure hadronic origin,  $\gamma$ -rays are predicted to be produced in the ICM as well (e.g., [33] and sections below). If this  $\gamma$ -ray emission is correlated with the radio emission, it can be used to derive the local magnetic field strengths [64]:

$$\frac{L_{\text{radio}}}{L_{\gamma}} \propto \left\langle \frac{B^{\alpha+1}}{B^2 + B_{\text{CMB}}^2} \right\rangle \tag{6}$$

In the equation above,  $L_{\text{radio}}$  and  $L_{\gamma}$  are the radio and  $\gamma$ -ray flux,  $\alpha$  is the radio spectral index,  $B$  is the magnetic field,  $B_{\text{CMB}}$  is the equivalent magnetic field of the CMB, and  $\langle \dots \rangle$  indicates the volume weighted quantity. However, so far no  $\gamma$ -ray emission could be unambiguously associated with the ICM (e.g., [65–70] and discussions below). However, even non-detection of  $\gamma$ -rays allows limits to be put on the magnetic fields in the ICM (e.g., [64,71]).

Another technique to measure cluster magnetic fields and their morphology is to study the rotation measure (RM) of polarised background sources (e.g., [72–74]). When propagating through the magnetised ICM, this polarised emission will be Faraday rotated—

i.e., the intrinsic polarisation angle at the source,  $\epsilon_{\text{int}}$ , will be rotated to the observed polarisation angle  $\epsilon_{\text{obs}}$  (e.g., [1] and references therein):

$$\epsilon_{\text{obs}} = \epsilon_{\text{int}} + \phi \lambda_{\text{obs}}^2. \quad (7)$$

The amount of rotation depends on the observing frequency,  $\nu_{\text{obs}} \propto 1/\lambda_{\text{obs}}$ , and the Faraday depth:

$$\phi \propto \int n_e B_{\parallel} d\text{los}. \quad (8)$$

The Faraday depth solely depends on the electron density  $n_e$  and the magnetic field component parallel to the line-of-sight  $B_{\parallel}$ . Consequently, if the polarised source is observed at multiple frequencies, one can constrain  $\phi$  and, hence,  $B_{\parallel}$ , provided that a model for the electron density is available. However, Faraday rotation measurements have to be performed with great caution [75]. As seen in Equations (7) and (8), at least three frequencies are required to remove the “ $\epsilon_{\text{obs}} = \epsilon_{\text{obs}} + n\pi$ -ambiguity”, and to properly derive the Faraday depth. Moreover, multiple Faraday screens or polarised background sources can pollute the observations. Therefore, several techniques such as RM synthesis, QU-fitting, or Faraday tomography have been developed (e.g., [10,12,15,76]).

Finally, the diffuse radio sources are predicted to be polarised as well. As we will discuss below, radio relics have been well studied in polarisation. On the other hand, radio halos are predicted to be polarised, but this polarised emission has yet to be observed. Nevertheless, the polarised emission can be used to directly study the magnetic field and its orientation in the plane-of-the-sky [63]. However, polarisation studies also pose some technical challenges. The polarised emission will also undergo Faraday rotation. As seen in Equation (8), the amount of Faraday rotation depends on the observing frequency. Specifically, low-frequency emission will undergo more Faraday rotation and, hence, more internal and external Faraday depolarisation. Vice versa, high-frequency emission will undergo less Faraday rotation and, hence, less depolarisation. Therefore, high-frequency studies of polarised emission are favoured. Yet, due to the spectral properties of the radio emission, high-frequency emission is fainter and most sources are detected at low frequencies. However, thanks to improving instruments and observational techniques we have started to detect polarised low-frequency emission as well [77]. Furthermore, there have been attempts to apply the stacking technique to polarised low-frequency emission [29,78].

#### 4. The Evolution of Magnetic Fields

The origin of magnetic fields in the Universe is still unknown and two scenarios have been proposed: the *primordial* scenario and the *astrophysical* scenario [5,9]. In the astrophysical scenario, magnetic fields are injected on galactic scales and they are transported to larger scales. Feedback from active galactic nuclei, galactic feedback, or star formation driven winds are mechanisms that can inject magnetic fields on galactic scales (e.g., [79] and references therein). In the primordial scenario, magnetic fields were created in the early Universe, e.g., possibly during baryogenesis, phase transition, or inflation (e.g., [5] and references therein).

In the end, the astrophysical scenario and the primordial scenario are not competing scenarios but they can also co-exist. However, in galaxy clusters, the two scenarios cannot be distinguished, as dynamo action erases any information on the primordial magnetic fields. Hence, to prove the existence of primordial magnetic fields, one has to study the less dense regions of the Universe—namely, cosmic filaments and voids. However, these regions are vastly unexplored and only recently have studies started to explore them [25–28].

Regardless of their exact origin, the magnetic seed fields are amplified by various processes during structure formation. The main drivers of magnetic field amplification are

turbulent motions that amplify the magnetic field via the small-scale dynamo (e.g., [80] and references therein). In the small-scale dynamo, the turbulent velocity field stretches and folds the pre-existing magnetic field lines, effectively amplifying the magnetic field due to flux conservation (e.g., [81,82]). In the high- $\beta$  regime, the magnetic flux is conserved and, consequently, if a flux tube is stretched from length  $l_1$  to length  $l_2$ , the magnetic field is amplified as:  $B_2 = B_1 \cdot (l_2/l_1)$ . The repetition of this process leads to an exponential amplification of the magnetic field, providing efficient magnetic field amplification. However, this exponential magnetic field amplification is only efficient as long as the magnetic field does not back react on the fluid—which is the case for weak magnetic seed fields. Once the magnetic field starts to back react on the fluid, the exponential growth stops and the dynamo enters the non-linear regime. In the non-linear regime, the magnetic field grows until it reaches equipartition with the turbulent kinetic energy.

Except turbulence and the small-scale dynamo there are several other processes that can amplify magnetic fields. However, none of these processes is as efficient as the small-scale dynamo. Hence, they can be seen as additional mechanisms that come on top of the small-scale dynamo but that cannot replace it. These additional mechanisms include adiabatic compression, shock waves, and cold fronts.

In magneto hydrodynamics (MHD), the magnetic flux is conserved, which causes the magnetic field to scale with density, i.e.,  $B \propto \rho^{2/3}$  [83]. Consequently, the magnetic field is amplified if plasma is compressed. However, adiabatic compression can only explain the magnetic field amplification by a few orders of magnitude, which is not sufficient to explain the  $\mu\text{G}$  magnetic fields in galaxy clusters [84,85].

Shock waves can amplify magnetic fields by a number of different mechanisms. The most natural one appears to be shock compression, which amplifies the quasi-perpendicular component of the upstream magnetic field [86]. However, typical ICM shocks have Mach numbers of a few, and the corresponding amplification is small. For example, a Mach number 5 shock, which is already at the top end of what is observed in the ICM, would amplify the magnetic field by a factor of  $\sim 5$ . On the other hand, shock waves can also be a source of turbulence. If the pre-shock gas has inhomogeneities, turbulence can be injected by a shock, potentially driving a small-scale dynamo (e.g., [87]). Yet, this process is not well studied for cluster shocks. As shown by [86], self-generated vorticity at cluster shocks is most likely not able to drive a turbulent dynamo, and a significant amount of pre-shock turbulence is needed to explain the observed magnetic field strengths.

Cold fronts are the third “large-scale” motions that can amplify magnetic fields. It has been demonstrated that a gas cloud, which moves subsonically through the ICM, can stretch and amplify the magnetic field along the contact discontinuity. This process forms a layer of magnetic draping outside of the contact discontinuity [88]. Sloshing cold fronts are also associated with amplified magnetic layers but they occur on the inside of the contact discontinuity [58].

## 5. Radio Halos—Turbulent Re-Acceleration in the ICM

Radio halos are large-scale synchrotron emission that is observed in the central regions of galaxy clusters. Mostly, radio halos are found in merging galaxy clusters, and, normally, the synchrotron emission follows the X-ray emission of the thermal ICM.

Historically, two models have been proposed for the origin of radio halos. The first model is the hadronic model, where secondary cosmic-ray electrons are produced by hadronic collisions between cosmic-ray protons and thermal protons. The second model is the model of turbulent re-acceleration, where particles are re-accelerated by the MHD turbulence in the cluster. Several observations favour the turbulent re-acceleration model over the pure hadronic model. Yet, it is still uncertain to what extent hadronic processes might still play a role in the formation of radio halos.

### 5.1. Pure Hadronic Model of Radio Halos

In the pure hadronic model, cosmic-ray protons are accelerated in the ICM. Eventually, the cosmic-ray protons collide with the thermal protons of the ICM. These collisions produce charged and neutral pions. Then, these charged pions decay into muons that decay into positrons and electrons. It was suggested that the resulting electrons are responsible for the radio halo emission (e.g., [89–91]). However, observational evidence against the hadronic model is piling up.

First, in the hadronic model, the neutral pions decay into  $\gamma$ -rays. However, such a  $\gamma$ -ray signal has not been unambiguously observed. The search for diffuse  $\gamma$ -ray emission from galaxy clusters has been going on for nearly three decades now, either from space at energies of about 30 MeV to 300 GeV [65–67,92–95], or from the ground at energies of about 50 GeV to 10 TeV [71,96–99]. While very useful to constrain cluster scale particle acceleration [64,100], these searches have remained inconclusive. Only recently, three independent groups have reported  $\gamma$ -ray emission toward the Coma cluster with Fermi-LAT data [68–70]. While the emission is in line with the expectations from cosmic-ray protons interacting hadronically in the ICM, the signal cannot be unambiguously attributed to the ICM because of possible AGN contamination and the limited angular resolution and sensitivity of the instruments. Nevertheless, even in the case where all the  $\gamma$ -ray flux is attributed to the ICM, this is not sufficient to explain the radio emission in the pure hadronic model [69].

Second, low-frequency radio observations discovered a new type of radio halos, namely, the ultra-steep-spectrum radio halos (USSRH) (e.g., [101]). These USSRH cannot be explained by the hadronic model, simply because the required population of cosmic-ray protons would require an energy density that is significantly larger than the energy density of the thermal plasma. Consequently, the cluster would be dominated by non-thermal protons, which appears unrealistic.

All these findings argue against a pure hadronic origin of radio halos. However, it might still be possible that hadronic collisions contribute to a small fraction to the observed halo emission. In this case, halos are produced by a combination of turbulent re-acceleration and hadronic collisions. Moreover, it is still uncertain to what extent hadronic processes contribute seed particles to the turbulent re-acceleration.

### 5.2. Turbulent Re-Acceleration

In this scenario, the electrons interact stochastically with the turbulent waves/modes of the ICM. At every interaction, the particles either gain or lose energy. As head-on collisions, that give energy to the particles, have a higher probability, these collisions effectively increase the particles' energy. Nevertheless, this is a stochastic and slow process. Brunetti and Lazarian [36] derived a turbulent re-acceleration mechanism in compressible ICM turbulence. They discussed resonant and non-resonant interactions between the particles and the turbulent compressible modes.

In the resonant acceleration, gyroresonant interactions between the MHD waves and the particles affect the motions of the particles. More specifically, the compressible component of the magnetic field interacts with the particles through transit time damping (TTD) [102,103]. However, TTD only changes the momentum parallel to the magnetic field. Hence, in order to maintain the acceleration process, TTD requires isotropization of the particles. Particle-pitch angle scattering can provide the required isotropization. Particle-pitch angle scattering can be driven by electron firehose instabilities, cosmic-ray fluid instabilities, or other plasma effects [104–106]. The momentum diffusion coefficient of TTD is derived through first-order corrections to the particles' orbits due to small amplitude plasma turbulence [103], or from quasi linear theory [107]. Exact calculations for the properties of the ICM yield that TTD can systematically accelerate cosmic-ray electrons to the required energies on timescales of  $\sim 10^8$  years [36].

In the non-resonant acceleration, cosmic rays are accelerated by interactions between cosmic rays and compressible ICM turbulence [36]. Here, the compression or expansion of

the ICM changes the particles' momentum. Statistically, the particles travel more within regions of compression and, hence, they effectively gain energy. This also produces a Fermi II-type acceleration mechanism. In this regime, a slow and a fast diffusion limit exist. In the slow limit, the particle diffusion is slower than the wave period and, hence, the particles mainly interact with the small turbulent eddies. Vice versa, in the fast limit, particles diffuse out of the turbulent eddies faster than the eddies turnover and, hence, the particles interact mainly with the largest eddies. Nevertheless, Brunetti and Lazarian [36] showed that the non-resonant interaction in the ICM has a similar efficiency to the resonant interaction.

However, numerical simulations have shown that turbulence in the ICM is predominantly solenoidal. Moreover, the compressive part of ICM turbulence is expected to be partially dissipated into weak shocks [39,40,108], leaving less energy for the turbulent re-acceleration. Consequently, other scenarios have been proposed. Brunetti and Lazarian [109] proposed a scenario, where particles diffuse in super-Alfvénic incompressible turbulence, where they gain energy via the statistical interaction with the magnetic field lines in regions of reconnection and turbulent dynamo.

Despite the details of the acceleration mechanism, turbulent acceleration of thermal particles to relativistic energies is an inefficient and slow process [36]. Therefore, it has been proposed that turbulence rather re-accelerates a population of fossil cosmic-ray electrons that is already present in the cluster. This raises the question of where such a large and uniform population of cosmic rays—required to produce radio halos—originated from [18]. It has been proposed that previous events of shock acceleration or outbursts from radio galaxies could produce the required fossil population. Moreover, hadronic interaction could also contribute to the required fossil population. However, these are very localised processes and it is still unclear if they can fill enough of the clusters' volume.

The turbulent re-acceleration model is favoured for the origin of radio halos, as it can explain several observed features. Radio halos are predominantly found in merging galaxy clusters, i.e., clusters in a turbulent dynamical state [110–112]. Radio halos have complex spectral properties, including large-scale fluctuations of the radio spectral index across the halo [19,101,113–120]. The turbulent re-acceleration scenario predicts the existence of the recently discovered ultra-steep-spectrum radio halos (USSRH) (e.g., [101]). Moreover, the turbulent re-acceleration scenario makes several predictions, which we discuss in the following section.

In the turbulent re-acceleration model, a fraction of the merger's energy is dissipated into turbulence and, hence, into the re-acceleration. As the merger's energy depends on the colliding clusters' mass, the amount of synchrotron emission scales with the clusters' mass as well. As a consequence, there is a strong correlation between a cluster's mass and the halo's radio power, i.e., the occurrence of radio halos should increase in more massive systems [111,121].

Moreover, the turbulent re-acceleration, i.e., energising of cosmic rays, is balanced by the energy losses, e.g., due to synchrotron radiation. This implies a steepening of the integrated spectral index towards higher frequencies. Consequently, at GHz frequencies, halos should preferentially be detected in massive systems with on-going merger activities, and GHz detections should be rarer in less massive systems [122]. Vice versa, the occurrence rate of radio halos should increase at low, i.e., 100s of MHz, frequencies. At these low frequencies, the cosmic rays that are re-accelerated by less energetic mergers should become visible.

In the turbulent re-acceleration model, cosmic rays gain energy from the interaction with the turbulent motions in the ICM. As turbulence is best studied with X-ray observations (e.g., [123–128] and references there), it is obvious to study the correlation between the X-ray and radio emissions of radio halos (e.g., [101,117,129,130] and references therein). Especially, a study of the point-to-point correlation between the radio emission and X-ray emission allows us to study the acceleration mechanism and the magnetic field distribution in galaxy clusters [131–133]. The turbulent re-acceleration model predicts a sublinear

point-to-point correlation between the radio emission and X-ray emission (see discussion in [19]). Such a sublinear correlation has been observed in several radio halos [19,120].

As depicted by Rajpurohit et al. [134], our understanding of the origin of radio halos is still incomplete. Rajpurohit et al. [134] studied the peculiar radio halo in Abell 2256. On the one hand, they found a number of observational properties that are clearly in line with the turbulent re-acceleration mechanism. These include (1) an ultra-steep integrated radio spectrum, (2) a spectral index that differs across the halo regions and that steepens towards the outskirts, (3) a sublinear correlation between the radio emission and X-ray emission, and (4) underluminosity at high observing frequencies. On the other hand, other observed features cannot be explained by turbulent re-acceleration and additional modifications of the model are needed. These features include (1) a possible connection of the radio emission and the cluster's cold fronts, (2) a superlinear correlation between the radio emission and X-ray emission in the cluster core, (3) an ultra-steep radio spectrum in the cluster core, and (4) differences between the radio–X-ray correlation in different sub-regions of the cluster. Consequently, they state that not all the observed features can be explained by the proposed turbulent re-acceleration model.

### 5.3. Mega Radio Halos

With recent low-frequency radio observations, Cuciti et al. [135] detected so called mega radio halos. In four galaxy clusters, they found radio halo emission that extends into a volume that is 30 times larger than the volume filled by the classical radio halos; see Figure 2. These new observations suggest that turbulence and, hence, cosmic-ray acceleration and magnetic field amplification are also present in the outskirts of galaxy clusters and beyond. While the exact origin of these mega halos is yet unknown, they might occur more often than classical halos. Hence, mega radio halos could also be present in less massive and relaxed systems—i.e., systems that are not expected to host any radio halo emission.

Also the radio halos in the COMA cluster and in Abell 2255 have been found to be larger than previously estimated [120,136]. If more giant radio halos are detected, especially in clusters without a classical radio halo, they would prove the presence of low-energy cosmic rays in the entire cluster volume. Such a population of low-energy cosmic rays could provide the seed cosmic rays which are required in the turbulent re-acceleration model.

### 5.4. Polarisation

It is predicted that halos should be intrinsically polarised [137–139]. However, polarisation observations of radio halos are extremely challenging as the effect of beam depolarisation is large [140]. In three cases, polarised emission from a radio halo has been claimed, namely, in the galaxy clusters Abell 2255, Abell 523, and MACSJ0717.5+3745 [141–143]. However, in the case of MACSJ0717.5+3745, high-resolution observations revealed the presence of polarised filamentary structures—potentially with a shock origin—in front of the halo [144]. This observation highlights the challenges and difficulties of polarisation observations of diffuse radio sources. Hence, due to the complex nature of their diffuse radio emission, it is still to be determined if the halos in A2255 [141] and Abell 523 [143] are polarised, or if the signal is emitted by a polarised foreground source as well. Nevertheless, a firm detection of polarised emission from radio halos will ultimately constrain the magnetic power spectrum.

Sur et al. [145] and Basu and Sur [140] modelled the polarised emission from halos with turbulence in box simulations. They confirmed that halos are expected to be intrinsically polarised, but highlighted the difficulties of detecting any polarised emission due to beam depolarisation.

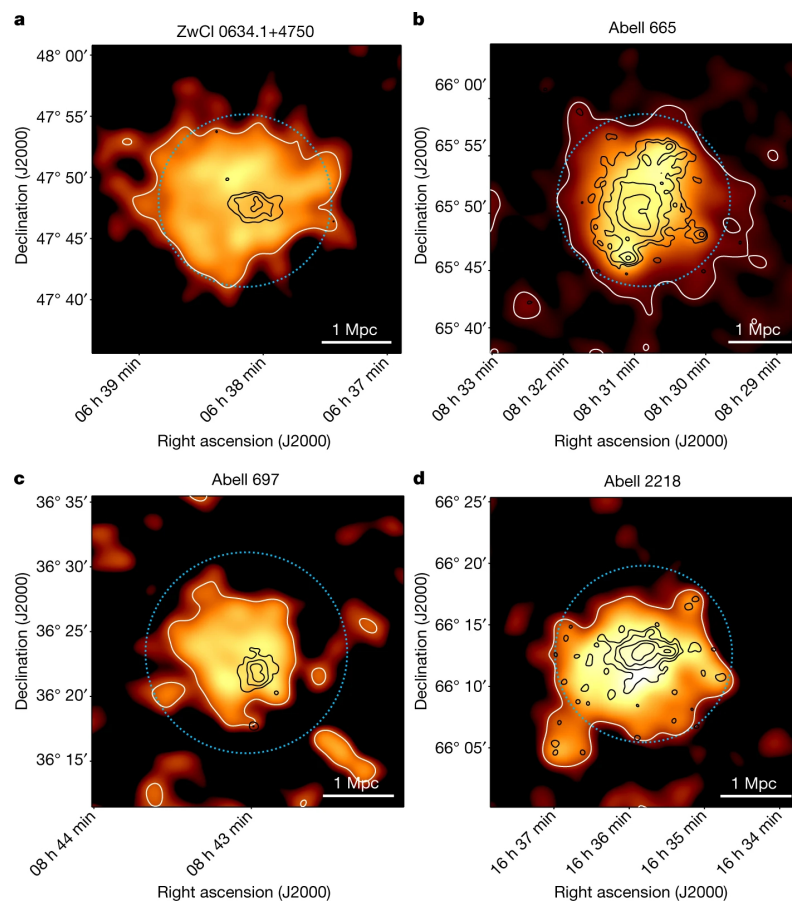


**Figure 2.** Mega radio halos detected by Cuciti et al. [135]: LOFAR 144 MHz observations of four galaxy clusters: (a) ZwCl 0634.1+4750, (b) Abell 665, (c) Abell 697, and (d) Abell 2218. The black contours show the location of the previously known radio halos. The white contours and orange colours show the 144 MHz observations at 2' resolution. In all four cases, the emission is significantly more extended than previously known. The extended emission even reaches beyond  $r_{500}$  (blue circle). Reproduced with permission from Cuciti et al.; published by Nature 2022.

### 5.5. High Redshifts

Most clusters hosting diffuse radio emission are located at redshifts below 0.5. Until recently, diffuse radio emission has only been studied in a few outstanding high-redshift clusters, i.e., clusters located above redshift 0.5. Using LOFAR, Di Gennaro et al. [146] detected diffuse radio emission in ten clusters located at redshifts above 0.6. The sample consists of nine radio halos and one radio relic, yielding a higher halo to relic ratio than in low redshift clusters. Follow up observations with the uGMRT detected only five of the high-redshift halos, indicating steep radio spectra, i.e., spectral indices of  $-1.4$  and even steeper for the clusters that are undetected at high frequencies [146].

This discovery of halos and relics suggests that magnetic field amplification and particle acceleration in high-redshift clusters must be of similar strengths as in low-redshift clusters, i.e., magnetic fields of a few  $\mu\text{G}$  and cosmic-ray electrons with about 100 MeV. On the other hand, the discovery raised several questions: How can clusters be highly magnetised at high redshifts? How efficient is the small-scale dynamo at these high redshifts? How can cosmic-ray acceleration be efficient in these dynamically young systems? Is turbulent re-acceleration more efficient than shock acceleration at high redshifts? All of these questions are yet unanswered, but answering them is relevant to understanding the origin and evolution of cosmic magnetic fields.

### 5.6. Basics of Mini-Halos

Radio mini-halos are smaller sized radio halos. However, they cannot be seen as the smaller version of the Mpc-size halos that were discussed above, because their origin and the properties of the host cluster are different. Normally, they are a few 100 kpc in size and they are exclusively found in relaxed cool-core clusters [147]. Moreover, their radio emission often surrounds the central AGN associated with the brightest cluster galaxy. As for radio halos, it has been proposed that radio mini-halos are either of hadronic origin or produced by turbulent (re-)acceleration.

The turbulent (re-)acceleration scenario is expected to be determined by similar plasma processes as described in Section 5.2. However, the turbulence is predicted to be induced by gas sloshing (e.g., [148–151] and references therein). The sloshing motions must induce large-scale turbulent motions while keeping the relaxed cool core intact. It was suggested that minor mergers and/or off-axis mergers could be a source of turbulence. This theory is supported by the observations of cold fronts that bound the mini-halos [57,152–154]. However, Savini et al. [155] have found faint, low-frequency emission beyond the cold fronts in RX J1720.1+2638. If this emission is also due to turbulence injected by a minor merger, that did not disrupt the cool-core, mini-halos and radio halos could potentially co-exist. The turbulent re-acceleration scenario for the origin of mini-halos also requires the existence of a seed population of fossil cosmic-ray electrons. The radio brightest central galaxy may provide a natural source of such a population of seed electrons [156]. This scenario is supported by an observed correlation between the radio powers of the mini-halo and the brightest cluster galaxies [157,158].

In the hadronic model of mini-halos, cosmic-ray electrons are again produced as a byproduct of the inelastic collisions between cosmic-ray protons and thermal protons of the ICM; see Section 5.1. The required population of cosmic-ray protons could originate from active galactic nuclei, in particular the brightest cluster galaxy, and supernovae processes. However, unlike for radio halos, the non-detection of  $\gamma$ -rays is still compatible with the hadronic origin of mini radio halos [159].

## 6. Radio Relics—Shock Acceleration in the ICM

Radio relics are the second big class of diffuse radio sources in the ICM. In the general picture, radio relics are arc-shaped sources that exist in the periphery of galaxy clusters [18]. Normally, they have a bright radio rim at their outer edge, followed by the dimming of radio emission towards the cluster centre. This gradient of radio emission comes along with a steepening of the spectral index, i.e., at the outer edge of the relic, the spectral index is flat, and it steepens towards the cluster centre. Consequently, particles must be accelerated at the outer edge of the relic and they age towards the cluster centre due to synchrotron emission. In most cases, radio relics are co-located with shock waves in the ICM that are detected in X-rays. This co-existence of relics and shock waves gave rise to the idea that relics are produced by the shock (re-)acceleration of cosmic-ray electrons [21].

### 6.1. Basics of Shock Acceleration

It is commonly accepted that radio relics are produced by the shock (re-)acceleration of cosmic-ray electrons (e.g., [21,160–166] and references therein). While the details of the acceleration mechanism—especially regarding the micro physics—are still to be worked out, it is generally assumed that *Diffusive Shock Acceleration* (DSA) is the acceleration mechanism at work (e.g., [33,34,167–169] and references therein).

In the basic picture of DSA, cosmic rays scatter off MHD waves/inhomogeneities that reside on both sides of the shock. This process temporarily traps the particles in a converging flow across the shock front, forcing the particles to cross the shock multiple times. At every shock crossing the cosmic rays gain energy, and eventually they escape the

shock by convecting downstream. This process produces a cosmic-ray energy spectrum that follows a power-law (e.g., [168]):

$$f(E) \propto E^{-\delta_{\text{inj}}}, \text{ with } \delta_{\text{inj}} = 2 \frac{M^2 + 1}{M^2 - 1}. \quad (9)$$

Here, the spectral index  $\delta_{\text{inj}}$  solely depends on the Mach number  $M$  of the shock wave. The beauty of this process is that the power-law of the energy spectrum directly translates into a power-law for the integrated radio spectrum, as observed for radio relics (e.g., [170,171]):

$$I_{\nu_{\text{obs}}} \propto \nu_{\text{obs}}^{-\alpha_{\text{int}}}, \text{ with } \alpha_{\text{int}} = \frac{M^2 + 1}{M^2 - 1}. \quad (10)$$

Consequently, the integrated radio spectrum contains information of the strength of the cosmic-ray accelerating shock.

DSA can explain several of the observed features of radio relics, especially several of the spectral properties. First of all, the observed radio spectra have power-law shapes that extend over several decades in frequency [170,172–174]. Moreover, the spectral steepening from the rim of the relic, i.e., the site of acceleration, into the downstream agrees very well with the expected ageing in the shock downstream [175–177]. Yet, there are some properties of radio relics that cannot be explained with DSA and we will discuss them in the following section.

## 6.2. Pre-Acceleration of Cosmic Rays

The biggest issue of the DSA framework to explain radio relics is the required acceleration efficiencies. Current models predict that the acceleration efficiencies for DSA from the thermal pool are below a few percent [178–188]. However, such efficiencies are too small to explain the observed luminosities of most radio relics, and they require an unrealistically large acceleration efficiency [189]. At the time of writing, only one relic is known that can be explained by DSA from the thermal pool [165].

To overcome this efficiency problem, it has been proposed that, in general, relics are produced by the re-acceleration of a pre-existing population of fossil cosmic-ray electrons. Such a population of fossil cosmic rays could have been produced by several processes, including the injection of cosmic rays by radio galaxies, the shock acceleration by previous merger events, and the energisation by sloshing motions [177,190–194].

In a pioneering work, Inchingolo et al. [192] used cosmological simulations to study the effect of multiple shocks accelerating cosmic-ray electrons in the outskirts of a galaxy cluster. They found that a significant fraction of cosmic-ray electrons ending up in a radio relic might have been pre-accelerated by previous shock passages. Moreover, this population of re-accelerated cosmic-ray electrons significantly contributes to the observed radio emission, explaining the high radio powers. However, they studied this *multi-shock scenario* for a single simulation, and it is still to be determined how likely this scenario is using a larger sample of simulations.

Radio galaxies could be an alternative source of fossil cosmic rays. This scenario is supported by the observation of radio galaxies in the vicinity of radio relics [175,190,191,195]. However, giant radio relics show a coherent radio emission across Mpc scales, and it is still unclear if a single radio galaxy—or several radio galaxies—is capable of producing the required large and uniform population of fossil electrons.

Using numerical simulations, ZuHone et al. [193] showed that sloshing motions, produced by AGN, can transport cosmic rays to the outskirts of galaxy clusters, where they can be re-accelerated by shocks. They also showed that the sloshing motions stretch the cosmic-ray population in a tangential direction, producing the elongated shape of radio relics. However, they also noted that this model is sensitive to the cosmic-ray physics in the ICM, and further investigations are needed.

Finally, it is possible that the cosmic rays undergo *shock drift acceleration (SDA)* at the shock [185,186,196]. In SDA, the cosmic rays that reside in the shock upstream drift along the shock front due to a gradient in the magnetic field. While drifting, the cosmic rays drain energy from a motional electric field. Eventually, the cosmic rays travel back into the upstream where they excite waves due to a temperature anisotropy. These waves scatter the cosmic rays back to the shock front, where the whole process is repeated. Guo et al. [185,186] have classified this process as a first-order Fermi process, which can energise the cosmic rays enough to allow them to undergo DSA.

As discussed above, it is still uncertain where a population of fossil cosmic-ray electrons might originate, and several viable scenarios have been proposed. Moreover, it is still unclear if one scenario alone could solve the efficiency problem for the whole population of radio relics. In fact, it appears rather unlikely that only one scenario is true. Fortunately, the different scenarios do not exclude each other. Hence, in nature it is most likely a combination of all the different scenarios.

### 6.3. The Shocks' Mach Numbers

Along with the acceleration efficiencies, it is also necessary to know the Mach numbers of shocks that are producing the relics. The Mach numbers of the shocks that produce radio relics can be derived from both X-ray observations (e.g., [37,197,198]) and radio observations (e.g., [175,199,200]). However, for several relics there is a mis-match between the two estimates, imposing a problem for the shock acceleration origin of radio relics [180,201–203,203–210].

Wittor et al. [211] have run a set of cosmological simulations to study this Mach number discrepancy. They found a mis-match between X-ray Mach numbers and radio Mach numbers that is comparable to the observed discrepancy. Moreover, they showed that this discrepancy is expected to appear naturally. Indeed, shocks that produce radio relics do not have a uniform Mach number but the Mach number varies across the shock front (e.g., [212–214]). Hence, a shock's strength is not characterised by a single Mach number but by a Mach number distribution. With a recent 2 Ms Chandra observation, Russell et al. [215] confirmed that the Mach number changes across the shock front in Abell 2146. Domínguez-Fernández et al. [216] showed that such a distribution arises naturally when a uniform shock travels into a turbulent or fluctuating medium. Wittor et al. [211] showed that the X-ray and radio Mach number trace two different parts of the underlying Mach number distribution. Here, the radio Mach number traces the high value tail of the distribution, while the X-ray Mach number rather characterises the distribution's average. Hence, the two measurements are expected to be intrinsically different.

Moreover, there are a few observational caveats that increase the Mach number discrepancy [211]. First, the X-ray Mach number is very sensitive to projection effects, and if the shock wave is not lying perfectly in the plane of the sky, it mostly underestimates the average of the Mach number distribution. Second, relics whose Mach number distribution extends more towards the high Mach numbers, are intrinsically brighter, and this high Mach number tail determines the radio Mach number. Hence, the Mach number discrepancy is larger for brighter radio relics. However, the brightest relics are the first relics to be detected. Hence, the Mach number discrepancy should vanish for fainter relics with steeper radio spectra that will be detected in the future.

### 6.4. Polarisation

In most cases, radio relics show a high degree of polarisation, whose origin was uncertain for a long time (e.g., [162,175,213,214,217–219] and references therein). The two competing scenarios were that the degree of polarisation is caused either by a magnetic field that is ordered on large scales, or by the compression and alignment of a magnetic field that is tangled on small scales [220]. In recent years, significant progress was made in understanding the polarisation of radio relics and, hence, of the magnetic fields at the shock front.

Di Gennaro et al. [221] presented high-resolution polarisation maps of the Sausage relic. These observations showed that the degree of polarisation is high at the edge of the relic and decreases in the downstream region. However, at first sight, this decrease appears counter-intuitive as the spectral index steepens in the downstream region. Theoretical models predict that for steeper spectral indices the degree of polarisation increases [60]. Specifically, for a population of cosmic-ray electrons that reside in a region with a homogeneous magnetic field, and that have a power-law energy distribution as in Equation (9), the intrinsic degree of polarisation  $p_0$  solely depends on the slope of the energy power-law  $\delta$ :

$$p_0 = \frac{3\delta + 3}{3\delta + 7} \quad (11)$$

As steeper radio spectral indices indicate steeper values for  $\delta$  (see Equation (2)) the intrinsic degree of polarisation would be expected to increase in the relics downstream. Hence, some mechanism must prohibit the degree of polarisation from increasing. Di Gennaro et al. [221] showed that projection effects can account for some part of the observation but they cannot explain the observed degree of polarisation. They suggested that only turbulent motions in the downstream region can explain the observations.

Simultaneously, Domínguez-Fernández et al. [222] studied the polarised emission of radio relics using a set of sophisticated simulations. They showed that ICM shocks are indeed able to align a turbulent magnetic field, producing the observed degree of polarisation at the shock front. Moreover, they found that the post-shock region still hosts enough turbulent motions to cause the degree of polarisation to rapidly decrease.

These findings have been used by Hoeft et al. [223] to derive an analytical model for the polarised emission of radio relics. This model yields the result that the shock compression scenario indeed provides a plausible explanation for the radio relic polarisation. Then, the depolarisation in the relic's downstream is caused by turbulent motions.

### 6.5. Lowest Radio Frequencies

Studying radio emission at the lowest radio frequencies, i.e., below 100 MHz, is of huge interest as they probe the oldest and low-energy cosmic-ray electrons. Hence, such observations contain significant information about the ageing processes at work. So far, only one observation of radio relics at ultra-low radio frequencies, i.e., below 100 MHz, has been performed. Using LOFAR LBA (39–78 MHz), de Gasperin et al. [224] studied the famous radio relic in the galaxy cluster RX J0603.3+4214; see Figure 3. They found that the relic emission extends up to 800 kpc into the downstream of the shock front. However, this distance is larger than what is allowed by the electron cooling time, i.e., 211 kpc. de Gasperin et al. [224] argue that the extended relic emission could be caused by two effects. First, downstream turbulence might re-accelerate the cosmic rays that travelled far into the downstream. Second, the radio relic is seen in projection with the radio halo in RX J0603.3+4214. In the future, it will be interesting to see how many radio relics show similar properties at frequencies below 100 MHz.

### 6.6. Shock Acceleration of Cosmic-Ray Protons

In principle, the shock waves that accelerate the electrons of the ICM are also expected to accelerate the protons of the ICM (e.g., [225] for a recent review). As in the pure hadronic model of radio halos (see Section 5.1) the shock-accelerated cosmic-ray protons eventually collide with the thermal ICM protons, producing  $\gamma$ -ray emission [226]. However, neither space-based observations nor ground-based observations have detected such a  $\gamma$ -ray signal (e.g., [65–67,71,94,97,99] and references therein). For several decades, this non-detection of  $\gamma$ -rays challenged our understanding of shock acceleration in the ICM. Hence, a significant amount of effort has been put forward to solve this problem of the “missing  $\gamma$ -rays”. The proposed solutions included modifications of the proton distribution in the ICM, revisions of the shock acceleration efficiencies, and a more detailed understanding of the

microphysical processes of the shock acceleration mechanism (e.g., [91,161,181,182,227–232] and references therein).

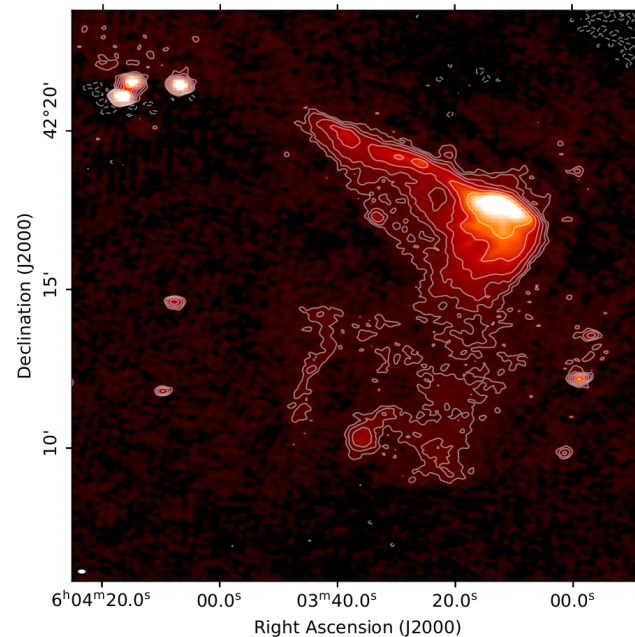


**Figure 3.** The radio relic in RX J0603.3+4214 observed at the lowest radio radio frequencies, i.e., 39–78 MHz, from de Gasperin et al. [224]. The downstream region of the brush extends much further into the downstream than previously observed with high-frequency observations. Reproduced with permission from de Gasperin et al.; published by A&A 2020.

Fortunately, thanks to the collaborative effort of observations, theory, and simulations, we are now able to explain the non-detection of  $\gamma$ -rays associated with the shock acceleration of cosmic-ray protons in the ICM. Theoretical studies showed that both the dynamical feedback of the cosmic-ray pressure on the shock and the energy dissipation due to Alfvén waves must be included in the calculation of the acceleration efficiencies [231]. Moreover, sophisticated numerical simulations showed that only quasi-parallel shocks, i.e., the angle between the shock normal and the underlying magnetic field is less than  $45^\circ$ , and only supercritical shocks, i.e., the shock’s Mach number must be above 2.25, are able to accelerate protons in the ICM [182,229]. Indeed, if all of these requirements are accounted for, the predicted  $\gamma$ -ray signals drop below the current upper limits given by observations [230,232].

Yet, it is noted that the constraints of the shock acceleration of cosmic-ray protons in the ICM do not affect the shock acceleration of cosmic-ray electrons. In fact, cosmic-ray electrons are predicted to be accelerated by different types of shock waves. Namely, only quasi-perpendicular shock waves, i.e., the angle between the shock normal and the underlying magnetic field is above  $45^\circ$ , are able to accelerate cosmic-ray electrons [185,186]. Moreover, the majority of shock waves in the ICM are predicted to be quasi-perpendicular [233–235]. Hence, it is more likely that cosmic-ray electrons are shock-accelerated in the ICM than cosmic-ray protons.

## 7. Beyond the Classical Radio Sources

With the continuous improvement of radio telescopes, as well as the exploration of the lowest radio frequencies, i.e., 100 MHz and below, we start to detect new radio sources that mostly consist of old fossil populations of cosmic rays (e.g., [129,236–239]). These sources, which come in different kinds of shapes, might have steep radio spectra and their origin is not entirely clear. In this final section, we want to briefly highlight the newest findings in the radio sky.

### 7.1. Gently Re-Energising Tails

Gently re-energising tails (GREets) are a new type of source that have been first detected in the galaxy cluster Abell 1033 at 142 MHz [240]. Ever since their first detection, other radio sources have been classified as GREets or are expected to be energised by a similar mechanism [241–243].

The proposed acceleration mechanisms for GREets is turbulent re-acceleration [240]. In this scenario, plasma instabilities, e.g., Rayleigh–Taylor or Kelvin–Helmholtz, generate turbulence in a confined region. This turbulence accelerates the cosmic-ray electrons via a second-order Fermi process to the required energies. Yet, it is still unclear how the turbulence and, hence, the re-acceleration process can be maintained in the confined volume over long timescales. Here, interactions between the confined volume and perturbations in the surrounding medium appear as a viable mechanism.

### 7.2. Remnant Sources

The low radio frequencies are of particular interest, as old and already aged cosmic-ray electrons are visible at these frequencies. Indeed, a significant number of observations have uncovered these old remnant sources (e.g., [129,236,238,239,241,244–246]). These old fossil sources are of high interest, as they directly give information on the age of the cosmic rays and, hence, on the ageing processes in the ICM. As synchrotron radiation is the dominant ageing process, these fossil sources give new insights on the magnetic field strengths in the ICM.

Some of these sources have spectacular morphologies; see Figure 4. In these cases, the corresponding cosmic-ray source cannot be determined, and the origin of the remnants remains unknown. In general, remnant sources might originate from radio galaxies or from some in situ acceleration mechanism in the ICM. On top of that, it is still to be determined if and how the magnetic field morphology shapes the remnants' morphologies.

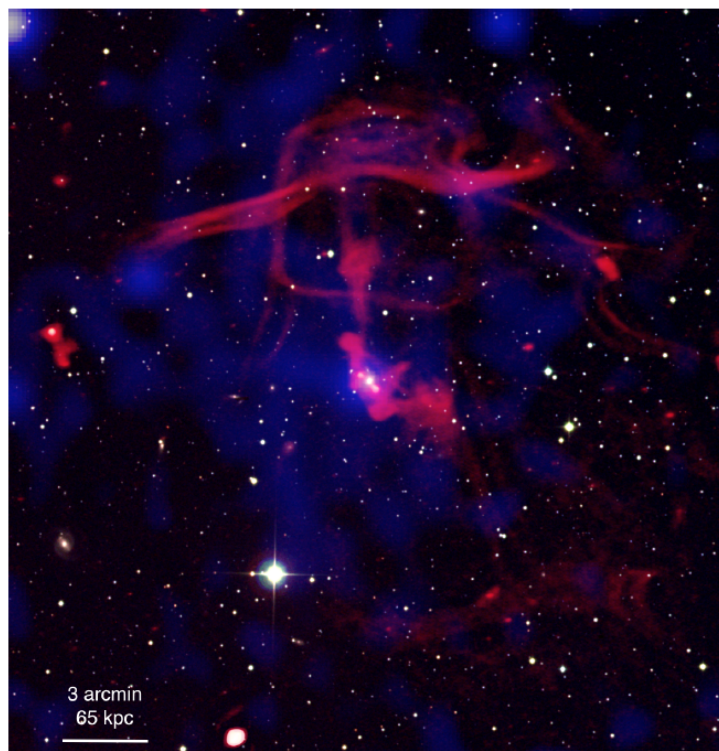


**Figure 4.** Complex non-thermal radio emission (red) in the galaxy group “Nest200047” observed by Brienza et al. [245]: These old fossil cosmic-ray electrons might provide the seeds for radio halos and radio relics. X-ray emission (blue) and optical data are shown in the background. Reproduced with permission from Brienza et al.; published by Nature Astronomy 2021.

The continuous detection of these remnant sources highlights the presence of a large number of fossil cosmic-ray electrons in the ICM that were previously invisible at high frequencies. Indeed, these fossils are required for the creation of both radio halos and radio relics, that are rather produced by the re-acceleration of fossil electrons than by the acceleration of thermal electrons.

### 7.3. Odd Radio Circles

Recently, a new type of diffuse radio source and, hence, sites of cosmic-ray acceleration has been discovered [247–250]. These sources have been named *odd radio circles (ORCs)*. The morphology of ORCs are closed circles of diffuse radio emission with diameters of a few 100 kpc. ORCs are similar to supernova remnants, but they do not have any optical and X-ray counterparts, arguing against the supernova origin. In addition to that fact, ORCs must be of extragalactic origin—most of them have been found between redshifts of 0.3 and 0.6—little is known about ORCs. Several competing theories to explain ORCs have been thought of [251–253]. They might be produced by shock waves driven by cataclysmic events, e.g., black hole mergers, in galaxies. Alternatively, shock waves could be driven by starburst winds, double loaded AGN seen end-on, or the interaction between galaxies. Even more exotic scenarios such as a connection to wormholes have been proposed [254,255]. While ORCs are not directly associated with galaxy clusters, they are the best evidence that not all particle accelerators in the Universe have been found. Hence, with the next generation of radio telescopes, we can expect to discover more new types of radio sources that will teach us about magnetic fields and cosmic-ray acceleration in the Universe.

## 8. Beyond Clusters: Cosmic Filaments and Voids

Magnetic fields and cosmic-ray electrons are expected to exist beyond the outskirts of galaxy clusters. They have been observed in intercluster bridges, and the observational evidence for their existence in cosmic filaments is piling up [8,29]. If magnetic fields are of primordial origin, they should also permeate the emptiest regions of the Universe, namely cosmic voids (e.g., [256]). For a detailed review about the regions beyond galaxy clusters, we point to the first review of this Special Issue.

### 8.1. Intercluster Bridges

Recently, diffuse radio emission has been detected in intercluster bridges, the space between two merging clusters [8,257,258]. Prior to the merging of two galaxy clusters, the gas between the two is compressed and heated, forming an intercluster bridge. Intercluster bridges are observable in X-rays. In intercluster bridges, several physical processes pre-process the ICM, and shape the resulting clusters. Shocks and turbulence might produce cosmic rays, that provide the seeds for radio relics and radio halos. Furthermore, magnetic fields might be already amplified by compression. The recent detection of intercluster bridges in radio provided new insights about cosmic-ray acceleration and magnetic field amplification in bridges. Figure 5 shows radio observations of the intercluster bridge in the merging system Abell 1758 [257].

Radio observations prove the acceleration of cosmic rays prior to the collision of the merger's components. Moreover, they suggest that magnetic fields of a few 0.1  $\mu\text{G}$  are already present in intercluster bridges. However, little is known about the exact processes leading to the radio emission in bridges. The absence of radio emission in some X-ray-detected bridges, that would be expected to emit in radio, underlines this lack of knowledge [259].

There is a consensus that several physical requirements are needed to form a radio-emitting intercluster bridge. First, a strong enough magnetic field of a few 0.1  $\mu\text{G}$  must be present. Second, a population of seed electrons that is being (re-)accelerated is needed. Third, these electrons must be (re-)accelerated by an in situ acceleration mechanism. Fourth, sufficient time to make bridges radio bright is required. However, the acceleration time must be shorter than the cooling time of the cosmic-ray electrons, i.e., below a few  $10^8$  years.

Only if all of these requirements are well understood is it possible to link the radio emission to the magnetic fields in bridges. To date, only three radio emitting bridges are known and, hence, all of the four ingredients are still unconstrained [8,257,258].

As bridges extend over several Mpc, the radio emitting cosmic-ray electrons must be accelerated in situ in bridges. Both shock acceleration and turbulent re-acceleration in the super-Alfvénic regime have been proposed [260]. While turbulent re-acceleration is slightly favoured over shock acceleration, the exact acceleration mechanism has yet to be determined. Nevertheless, both turbulent re-acceleration and shock acceleration require a population of seed cosmic rays. However, it is still unclear where these seeds could originate.

In intercluster bridges, magnetic field strengths are estimated to be less than  $1 \mu\text{G}$ . In principle, both dynamo action and compression might be responsible for the magnetic field amplification. Whatever the true amplification mechanism, it is yet to be determined if dynamo action and/or compression have enough time to amplify the magnetic fields.

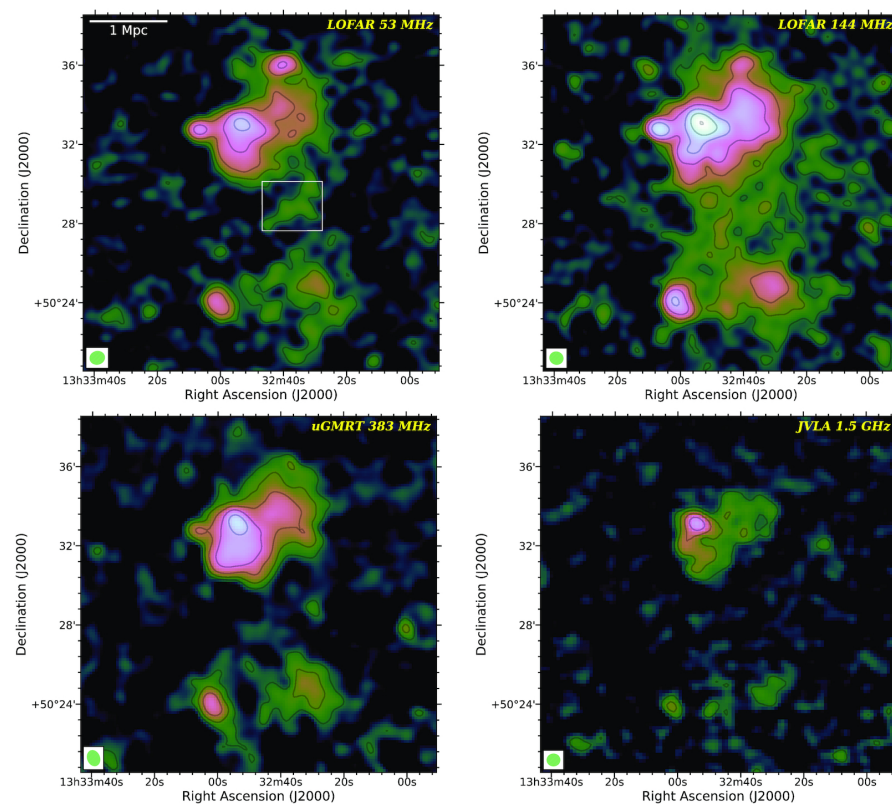


**Figure 5.** Diffuse radio emission inbetween Abell 1758N and Abell 1758S observed by Botteon et al. [257]: At 53 MHz and 144 MHz, diffuse radio emission is visible between the two clusters (**top** panels). This radio emission disappears at higher frequencies, i.e., 383 MHz and 1.5 GHz (**bottom** panels). Reproduced with permission from Botteon et al.; published by MNRAS 2020.

## 8.2. Cosmic Filaments and Voids

When studying the large-scale magnetic fields, cosmic filaments and voids belong to the most intriguing objects, as they will contain any signature of a primordial magnetic seed field. Unlike in clusters, dynamo amplification is expected to be inefficient in both filaments and voids. Therefore, magnetic fields are solely amplified via isotropic adiabatic compression and any imprints of a primordial seed field are preserved [6,7,17]. Consequently, a firm detection of magnetic fields in filaments or even in voids will ultimately prove the existence of a primordial magnetic field and solve the long-standing question of the origin of cosmic magnetism. As primordial seed fields are generated during the epochs preceding structure formation, their detection will also open a new window to indirectly probe the early Universe [261].

Limits on the magnetic fields strengths in filaments come mainly from the observations of Faraday rotation of polarised background radio galaxies [25–28]. These indirect measurements yield upper limits of a few nG. In principle, it is possible that radio-emitting filaments are directly observable. Numerical simulations have shown that strong accretion shocks are present in filaments [56]. These shocks can accelerate the electrons in filaments to the radio bright regime. However, due to the low gas densities,  $\sim 10^{-5}$ – $10^{-6}$  cm $^{-3}$ , and weak magnetic fields, such a signal would be very faint. Radio emission from cosmic filaments has been reported by Vacca et al. [262] and Vernstrom et al. [29]. In both cases, the corresponding magnetic fields are estimated to be of a few tens of nG.

Magnetic fields in filaments are predicted to be strongly aligned [235], and any radio signal should be highly polarised. Moreover, polarisation observations have a higher dynamical range, as any unpolarised sources will not pollute the observation [263]. In a pioneering work, Vernstrom et al. [264] stacked polarisation observations of cosmic filaments to detect such a signal. Indeed, they detected a polarisation fraction above 20%, which is explained by strong accretion shocks aligning the magnetic fields in the cluster's peripheries and inbetween the clusters.

In voids, limits on the magnetic fields are coming from blazar studies [265]. These studies suggest that the magnetic fields in voids range from  $10^{-16}$  G to  $10^{-10}$  G. These estimates agree with predictions for seed fields being produced during inflation or post-inflation. Moreover, magnetic field strengths of  $10^{-10}$  G can also be produced by astrophysical seeding, provided that the void galaxies are able to magnetise large enough fractions of a void's volume [256]. Narrowing the limits of the void magnetic fields will give new constraints on primordial magnetic seed fields. However, direct measurements of magnetic fields in cosmic voids remain challenging. Fortunately, RM signals from void galaxies can be used to estimate the void magnetic fields.

## 9. Summary

Cosmic magnetic fields and cosmic-ray acceleration are an important puzzle piece in understanding our Universe. Yet, our knowledge of both is still incomplete. Hence, it is obvious that the fields of cosmic magnetic fields and cosmic-ray acceleration are vivid and fast evolving. Especially, the recent technical advances in radio astronomy are a key player in the recent advances of the field. All the recent discoveries, presented in this work are just foreshadows of the new phenomena that are waiting to be discovered with the Square Kilometre Array (e.g., [266]).

The origin and evolution of cosmic magnetic fields is one of the most important and open issues in modern astrophysics [5,6]. Hence, deciphering both the origin and evolution of cosmic magnetic fields will provide new insights on the origin of the Universe. Moreover, cosmic magnetic fields play crucial roles in a variety of astrophysical phenomena that we could not discuss in this review. In galaxy clusters, magnetic fields and cosmic rays provide an additional pressure support that needs to be accounted for in cluster mass estimates, that are relevant in high-precision cosmology [267]. Moreover, they govern the transport of both the heat and momentum in the ICM, and they play crucial roles in a variety of plasma instabilities [268,269]. They are needed when searching for axion-like particles—one of the dark matter candidates—using cosmic birefringence [270,271]. Magnetic fields affect the acceleration and propagation of ultra-high-energy cosmic rays, especially in filaments and cosmic voids [235,272,273]. A detection of primordial magnetic fields, that are generated during the epochs preceding structure formation, will also open a new window to indirectly probe the early Universe. This new window to the early Universe might ultimately solve the Hubble tension [261]. Finally, magnetic fields provide new insights into the fundamentals of plasma physics itself. For example, understanding the evolution of cosmic magnetic fields will help us to better understand the physics of the small-scale dynamo [274]. Hence, a better knowledge of cosmic magnetic fields will ultimately lead to a better understanding of these different processes.

Extragalactic cosmic-ray electrons can be seen as the messengers that provide us with information about cosmic magnetic fields [33,34]. Hence, it is essential to study the physics of cosmic-ray acceleration in the Universe. However, the importance of understanding cosmic-ray acceleration in galaxy clusters and beyond is not to be belittled. In fact, the plasma conditions—a hot and ionised high  $\beta$ -plasma—that are present in the ICM and the cosmic web are not reproducible on Earth. Hence, the ICM and the cosmic web will remain our only laboratories to study cosmic-ray acceleration under these conditions.

As highlighted above, radio observations, paired with sophisticated numerical simulations, are our most powerful tool to observe and study magnetic fields and cosmic-ray acceleration in galaxy clusters, cosmic filaments, and cosmic voids. Fortunately, we are entering the golden age of radio astronomy. The new generation of radio telescopes, e.g., LOFAR, ASKAP, and MeerKAT, has started to explore the radio sky [275–279]. Moreover, the generation of older radio telescopes, e.g., VLA and GMRT, have undergone significant upgrades [280–282]. These technical advances have resulted in unprecedented detailed observations. Figure 6 provides a taste of the capabilities of these new radio facilities.

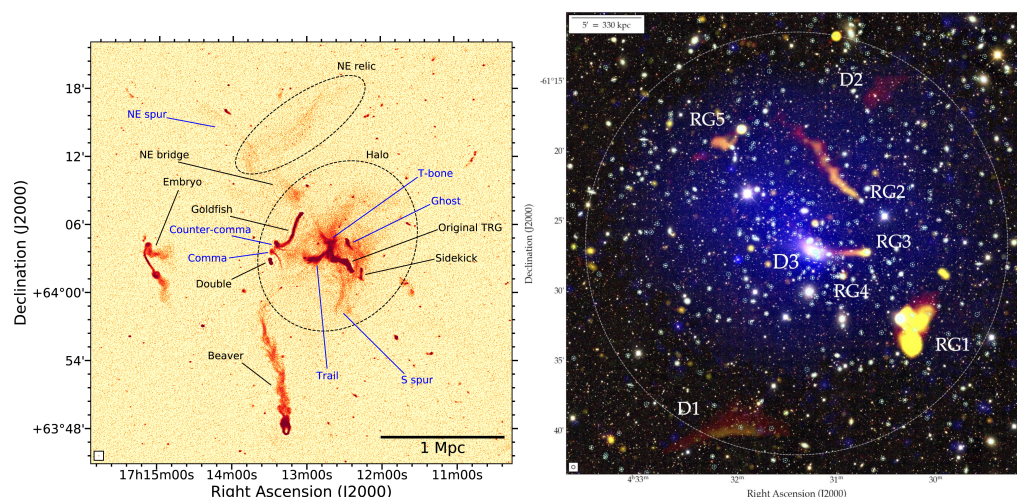


**Figure 6.** LOFAR observation of the galaxy cluster Abell 2255 (left) by Botteon et al. [119], and ASKAP–EMU observation of the galaxy cluster Abell 3266 (right) by Riseley et al. [129]. The two figures show the huge diversity of different radio sources that are being detected with the new generation of radio telescopes. For detailed descriptions of the different sources we point to the references. Reproduced with permission from Botteon et al.; published by ApJ 2020. Reproduced with permission from Riseley et al.; published by MNRAS 2022.

Radio astronomy is stepping into a golden future. We have just started to fully exploit the capabilities of the different radio facilities, and new discoveries are made everyday. These new observations shed new light on the cosmic-ray acceleration processes and magnetic fields in the Universe. In fact, the study of the polarised and unpolarised radio sky across the whole radio frequency band will allow us to derive a three-dimensional picture of the cosmic magnetic fields.

**Funding:** D.W. was funded by the Deutsche Forschungsgemeinschaft (DFG, German Research Foundation)—441694982.

**Data Availability Statement:** No data has been used in the work.

**Acknowledgments:** The author would like to thank K. Rajpurohit, V. Cuciti, F. de Gasperin, M. Brienza, A. Botteon, and C. Riseley for providing the figures associated with their work. Furthermore, the author would like to apologise to all scientists, whose work could not be covered in this review. The discussed field is fast evolving, and it is almost impossible to summarise all these works. Furthermore, the author would like to thank all his collaborators for great scientific collaborations and fruitful discussions about the topic. Finally, the author would like to thank the referees for their constructive report and criticism.

**Conflicts of Interest:** The author declares no conflict of interest. The funders had no role in the design of the study; in the collection, analyses, or interpretation of the data; in the writing of the manuscript; or in the decision to publish this work.

## Notes

- <sup>1</sup> In principle, also cosmic-ray protons could be present in the Universe. However, they have never been unambiguously observed. Throughout this paper, we use cosmic-ray electrons and cosmic rays interchangeably. We state explicitly when we are talking about cosmic-ray protons.
- <sup>2</sup> To put this fast evolution of the field into numbers, according to the ADS abstract service, in the period 2000 to 2009, 47 papers were published that contained the word “radio relic” in the abstract. Between 2010 and 2019, this number increased to 212, and, between 2020 and 2022, already 69 such papers have been published. Similar numbers are found when searching for “radio halo”. Here, the number of papers increased from 157 (period 2000–2009) to 282 (period 2010–2019). Between 2020 and 2022, 83 such papers have been published.

## References

1. Klein, U.; Fletcher, A. *Galactic and Intergalactic Magnetic Fields*; Springer: Berlin/Heidelberg, Germany, 2015.
2. Sarazin, C.L. The Physics of Cluster Mergers. In *Merging Processes in Galaxy Clusters*; Feretti, L., Gioia, I.M., Giovannini, G., Eds.; Astrophysics and Space Science Library; Springer: Berlin/Heidelberg, Germany, 2002; Volume 272, pp. 1–38. [[CrossRef](#)]
3. Schneider, P. *Extragalactic Astronomy and Cosmology*; Springer: Berlin/Heidelberg, Germany, 2006.
4. Planelles, S.; Schleicher, D.R.G.; Bykov, A.M. Large-Scale Structure Formation: From the First Non-linear Objects to Massive Galaxy Clusters. *Space Sci. Rev.* **2015**, *188*, 93–139. [[CrossRef](#)]
5. Subramanian, K. The origin, evolution and signatures of primordial magnetic fields. *Rep. Prog. Phys.* **2016**, *79*, 076901. [[CrossRef](#)] [[PubMed](#)]
6. Donnert, J.; Vazza, F.; Brüggem, M.; ZuHone, J. Magnetic Field Amplification in Galaxy Clusters and Its Simulation. *Space Sci. Rev.* **2018**, *214*, 122. [[CrossRef](#)]
7. Vazza, F.; Locatelli, N.; Rajpurohit, K.; Banfi, S.; Domínguez-Fernández, P.; Wittor, D.; Angelinelli, M.; Inchingolo, G.; Brienza, M.; Hackstein, S.; et al. Magnetogenesis and the Cosmic Web: A Joint Challenge for Radio Observations and Numerical Simulations. *Galaxies* **2021**, *9*, 109. [[CrossRef](#)]
8. Govoni, F.; Orrù, E.; Bonafede, A.; Iacobelli, M.; Paladino, R.; Vazza, F.; Murgia, M.; Vacca, V.; Giovannini, G.; Feretti, L.; et al. A radio ridge connecting two galaxy clusters in a filament of the cosmic web. *Science* **2019**, *364*, 981–984. [[CrossRef](#)]
9. Cho, J. Origin of Magnetic Field in the Intracluster Medium: Primordial or Astrophysical? *Astrophys. J.* **2014**, *797*, 133. [[CrossRef](#)]
10. Brentjens, M.A.; de Bruyn, A.G. Faraday rotation measure synthesis. *Astron. Astrophys.* **2005**, *441*, 1217–1228. [[CrossRef](#)]
11. Ferrari, C.; Govoni, F.; Schindler, S.; Bykov, A.M.; Rephaeli, Y. Observations of Extended Radio Emission in Clusters. *Space Sci. Rev.* **2008**, *134*, 93–118. [[CrossRef](#)]
12. Bell, M.R.; Enßlin, T.A. Faraday synthesis. The synergy of aperture and rotation measure synthesis. *Astron. Astrophys.* **2012**, *540*, A80. [[CrossRef](#)]
13. Feretti, L.; Giovannini, G.; Govoni, F.; Murgia, M. Clusters of galaxies: Observational properties of the diffuse radio emission. *Astron. Astrophys. Rev.* **2012**, *20*, 54. [[CrossRef](#)]
14. Govoni, F.; Johnston-Hollitt, M.; Agudo, I.; Akahori, T.; Beck, R.; Bonafede, A.; Carozzi, T.D.; Colafrancesco, S.; Feretti, L.; Ferriere, K.; et al. Cosmic Magnetism Science in the SKA1 Era. Square Kilometre Array Organisation Science Working Group Assessment Workshop Summary, NO. 6, Cosmic Magnetism, 26 Pages. Published Online by the SKA Organisation, March 2014. 2014. Available online: [https://indico.skatelescope.org/event/274/attachments/1958/2463/Magnetism\\_SAW\\_Memo\\_8Feb2014.pdf](https://indico.skatelescope.org/event/274/attachments/1958/2463/Magnetism_SAW_Memo_8Feb2014.pdf) (accessed on 26 June 2023).
15. Rudnick, L.; Katz, D.; Sebokolodi, L. Polarization Tomography with Stokes Parameters. *Galaxies* **2021**, *9*, 92. [[CrossRef](#)]
16. Vachaspati, T. Progress on cosmological magnetic fields. *Rep. Prog. Phys.* **2021**, *84*, 074901. [[CrossRef](#)] [[PubMed](#)]
17. Locatelli, N.; Vazza, F.; Bonafede, A.; Banfi, S.; Bernardi, G.; Gheller, C.; Botteon, A.; Shimwell, T. New constraints on the magnetic field in cosmic web filaments. *Astron. Astrophys.* **2021**, *652*, A80. [[CrossRef](#)]
18. van Weeren, R.J.; de Gasperin, F.; Akamatsu, H.; Brüggem, M.; Feretti, L.; Kang, H.; Stroe, A.; Zandanel, F. Diffuse Radio Emission from Galaxy Clusters. *Space Sci. Rev.* **2019**, *215*, 16. [[CrossRef](#)]
19. Rajpurohit, K.; Vazza, F.; van Weeren, R.J.; Hoeft, M.; Brienza, M.; Bonnassieux, E.; Riseley, C.J.; Brunetti, G.; Bonafede, A.; Brüggem, M.; et al. Dissecting nonthermal emission in the complex multiple-merger galaxy cluster Abell 2744: Radio and X-ray analysis. *Astron. Astrophys.* **2021**, *654*, A41. [[CrossRef](#)]
20. Jaffe, W.J. Origin and transport of electrons in the halo radio source in the Coma cluster. *Astrophys. J.* **1977**, *212*, 1–7. [[CrossRef](#)]
21. Ensslin, T.A.; Biermann, P.L.; Klein, U.; Kohle, S. Cluster radio relics as a tracer of shock waves of the large-scale structure formation. *Astron. Astrophys.* **1998**, *332*, 395–409.
22. Brunetti, G.; Setti, G.; Feretti, L.; Giovannini, G. Particle reacceleration in the Coma cluster: Radio properties and hard X-ray emission. *Mon. Not. R. Astron. Soc.* **2001**, *320*, 365–378. [[CrossRef](#)]

23. Petrosian, V. On the Nonthermal Emission and Acceleration of Electrons in Coma and Other Clusters of Galaxies. *Astrophys. J.* **2001**, *557*, 560–572. [[CrossRef](#)]
24. Gitti, M.; Brunetti, G.; Setti, G. Modeling the interaction between ICM and relativistic plasma in cooling flows: The case of the Perseus cluster. *Astron. Astrophys.* **2002**, *386*, 456–463. [[CrossRef](#)]
25. Vernstrom, T.; Gaensler, B.M.; Rudnick, L.; Andernach, H. Differences in Faraday Rotation between Adjacent Extragalactic Radio Sources as a Probe of Cosmic Magnetic Fields. *Astrophys. J.* **2019**, *878*, 92. [[CrossRef](#)]
26. O’Sullivan, S.P.; Brügggen, M.; Vazza, F.; Carretti, E.; Locatelli, N.T.; Stuardi, C.; Vacca, V.; Vernstrom, T.; Heald, G.; Horellou, C.; et al. New constraints on the magnetization of the cosmic web using LOFAR Faraday rotation observations. *Mon. Not. R. Astron. Soc.* **2020**, *495*, 2607–2619. [[CrossRef](#)]
27. Xu, J.; Han, J.L. Evidence for Strong Intracluster Magnetic Fields in the Early Universe. *Astrophys. J.* **2022**, *926*, 65. [[CrossRef](#)]
28. Carretti, E.; O’Sullivan, S.P.; Vacca, V.; Vazza, F.; Gheller, C.; Vernstrom, T.; Bonafede, A. Magnetic field evolution in cosmic filaments with LOFAR data. *Mon. Not. R. Astron. Soc.* **2023**, *518*, 2273–2286. [[CrossRef](#)]
29. Vernstrom, T.; Heald, G.; Vazza, F.; Galvin, T.J.; West, J.L.; Locatelli, N.; Fornengo, N.; Pinetti, E. Discovery of magnetic fields along stacked cosmic filaments as revealed by radio and X-ray emission. *Mon. Not. R. Astron. Soc.* **2021**, *505*, 4178–4196. [[CrossRef](#)]
30. Hodgson, T.; Vazza, F.; Johnston-Hollitt, M.; McKinley, B. Stacking the synchrotron cosmic web with FIGARO. *Publ. Astron. Soc. Aust.* **2022**, *39*, e033. [[CrossRef](#)]
31. Subramanian, K.; Shukurov, A.; Haugen, N.E.L. Evolving turbulence and magnetic fields in galaxy clusters. *Mon. Not. R. Astron. Soc.* **2006**, *366*, 1437–1454. [[CrossRef](#)]
32. Brügggen, M.; Bykov, A.; Ryu, D.; Röttgering, H. Magnetic Fields, Relativistic Particles, and Shock Waves in Cluster Outskirts. *Space Sci. Rev.* **2012**, *166*, 187–213. [[CrossRef](#)]
33. Brunetti, G.; Jones, T.W. Cosmic Rays in Galaxy Clusters and Their Nonthermal Emission. *Int. J. Mod. Phys. D* **2014**, *23*, 1430007–1430098. [[CrossRef](#)]
34. Bykov, A.M.; Vazza, F.; Kropotina, J.A.; Levenfish, K.P.; Paerels, F.B.S. Shocks and Non-thermal Particles in Clusters of Galaxies. *Space Sci. Rev.* **2019**, *215*, 14. [[CrossRef](#)]
35. Simionescu, A.; ZuHone, J.; Zhuravleva, I.; Churazov, E.; Gaspari, M.; Nagai, D.; Werner, N.; Roediger, E.; Canning, R.; Eckert, D.; et al. Constraining Gas Motions in the Intra-Cluster Medium. *Space Sci. Rev.* **2019**, *215*, 24. [[CrossRef](#)]
36. Brunetti, G.; Lazarian, A. Compressible turbulence in galaxy clusters: Physics and stochastic particle re-acceleration. *Mon. Not. R. Astron. Soc.* **2007**, *378*, 245–275. [[CrossRef](#)]
37. Markevitch, M.; Vikhlinin, A. Shocks and cold fronts in galaxy clusters. *Phys. Rep.* **2007**, *443*, 1–53. [[CrossRef](#)]
38. Vazza, F.; Brunetti, G.; Kritsuk, A.; Wagner, R.; Gheller, C.; Norman, M. Turbulent motions and shocks waves in galaxy clusters simulated with adaptive mesh refinement. *Astron. Astrophys.* **2009**, *504*, 33–43. [[CrossRef](#)]
39. Miniati, F. The Matryoshka Run: A Eulerian Refinement Strategy to Study the Statistics of Turbulence in Virialized Cosmic Structures. *Astrophys. J.* **2014**, *782*, 21. [[CrossRef](#)]
40. Miniati, F. The Matryoshka Run. II. Time-dependent Turbulence Statistics, Stochastic Particle Acceleration, and Microphysics Impact in a Massive Galaxy Cluster. *Astrophys. J.* **2015**, *800*, 60. [[CrossRef](#)]
41. Beresnyak, A.; Miniati, F. Turbulent Amplification and Structure of the Intracluster Magnetic Field. *Astrophys. J.* **2016**, *817*, 127. [[CrossRef](#)]
42. Vazza, F.; Jones, T.W.; Brügggen, M.; Brunetti, G.; Gheller, C.; Porter, D.; Ryu, D. Turbulence and vorticity in Galaxy clusters generated by structure formation. *Mon. Not. R. Astron. Soc.* **2017**, *464*, 210–230. [[CrossRef](#)]
43. Wittor, D.; Jones, T.; Vazza, F.; Brügggen, M. Evolution of vorticity and enstrophy in the intracluster medium. *Mon. Not. R. Astron. Soc.* **2017**, *471*, 3212–3225. [[CrossRef](#)]
44. Vazza, F.; Brunetti, G.; Gheller, C.; Brunino, R.; Brügggen, M. Massive and refined. II. The statistical properties of turbulent motions in massive galaxy clusters with high spatial resolution. *Astron. Astrophys.* **2011**, *529*, A17. [[CrossRef](#)]
45. Cassano, R.; Brunetti, G. Cluster mergers and non-thermal phenomena: A statistical magneto-turbulent model. *Mon. Not. R. Astron. Soc.* **2005**, *357*, 1313–1329. [[CrossRef](#)]
46. Liu, W.; Sun, M.; Nulsen, P.; Clarke, T.; Sarazin, C.; Forman, W.; Gaspari, M.; Giacintucci, S.; Lal, D.V.; Edge, T. AGN feedback in galaxy group 3C 88: Cavities, shock, and jet reorientation. *Mon. Not. R. Astron. Soc.* **2019**, *484*, 3376–3392. [[CrossRef](#)]
47. Gaspari, M.; Tombesi, F.; Cappi, M. Linking macro-, meso- and microscales in multiphase AGN feeding and feedback. *Nat. Astron.* **2020**, *4*, 10–13. [[CrossRef](#)]
48. Wittor, D.; Gaspari, M. Dissecting the turbulent weather driven by mechanical AGN feedback. *Mon. Not. R. Astron. Soc.* **2020**, *498*, 4983–5002. [[CrossRef](#)]
49. Kolmogorov, A. The Local Structure of Turbulence in Incompressible Viscous Fluid for Very Large Reynolds’ Numbers. *Akad. Nauk. SSSR Dokl.* **1941**, *30*, 301–305.
50. Hitomi Collaboration. The quiescent intracluster medium in the core of the Perseus cluster. *Nature* **2016**, *535*, 117–121. [[CrossRef](#)]
51. Ha, J.H.; Ryu, D.; Kang, H. Properties of Merger Shocks in Merging Galaxy Clusters. *Astrophys. J.* **2018**, *857*, 26. [[CrossRef](#)]
52. Gu, L.; Akamatsu, H.; Shimwell, T.W.; Intema, H.T.; van Weeren, R.J.; de Gasperin, F.; Mernier, F.; Mao, J.; Urdampilleta, I.; de Plaa, J.; et al. Observations of a pre-merger shock in colliding clusters of galaxies. *Nat. Astron.* **2019**, *3*, 838–843. [[CrossRef](#)]
53. Zhang, C.; Churazov, E.; Forman, W.R.; Lyskova, N. Runaway merger shocks in galaxy cluster outskirts and radio relics. *Mon. Not. R. Astron. Soc.* **2019**, *488*, 5259–5266. [[CrossRef](#)]

54. Zhang, C.; Churazov, E.; Dolag, K.; Forman, W.R.; Zhuravleva, I. Collision of merger and accretion shocks: Formation of Mpc-scale contact discontinuity in the Perseus cluster. *Mon. Not. R. Astron. Soc.* **2020**, *498*, L130–L134. [[CrossRef](#)]
55. Zhang, C.; Churazov, E.; Zhuravleva, I. Pairs of giant shock waves (N-waves) in merging galaxy clusters. *Mon. Not. R. Astron. Soc.* **2021**, *501*, 1038–1045. [[CrossRef](#)]
56. Ryu, D.; Kang, H.; Hallman, E.; Jones, T.W. Cosmological Shock Waves and Their Role in the Large-Scale Structure of the Universe. *Astrophys. J.* **2003**, *593*, 599–610. [[CrossRef](#)]
57. Ghizzardi, S.; Rossetti, M.; Molendi, S. Cold fronts in galaxy clusters. *Astron. Astrophys.* **2010**, *516*, A32. [[CrossRef](#)]
58. Zuhone, J.A.; Roediger, E. Cold fronts: Probes of plasma astrophysics in galaxy clusters. *J. Plasma Phys.* **2016**, *82*, 535820301. [[CrossRef](#)]
59. Zinger, E.; Dekel, A.; Birnboim, Y.; Nagai, D.; Lau, E.; Kravtsov, A.V. Cold fronts and shocks formed by gas streams in galaxy clusters. *Mon. Not. R. Astron. Soc.* **2018**, *476*, 56–70. [[CrossRef](#)]
60. Rybicki, G.B.; Lightman, A.P. *Radiative Processes in Astrophysics*; John Wiley & Sons: Hoboken, NJ, USA, 1986.
61. Beck, R.; Krause, M. Revised equipartition and minimum energy formula for magnetic field strength estimates from radio synchrotron observations. *Astron. Nachrichten* **2005**, *326*, 414–427. [[CrossRef](#)]
62. Rephaeli, Y.; Nevalainen, J.; Ohashi, T.; Bykov, A.M. Nonthermal Phenomena in Clusters of Galaxies. *Space Sci. Rev.* **2008**, *134*, 71–92. [[CrossRef](#)]
63. Mirakhor, M.S.; Walker, S.A.; Runge, J.; Diwanji, P. Possible non-thermal origin of the hard X-ray emission in the merging galaxy cluster SPT-CL J2031-4037. *Mon. Not. R. Astron. Soc.* **2022**, *516*, 1855–1864. [[CrossRef](#)]
64. Brunetti, G.; Zimmer, S.; Zandanel, F. Relativistic protons in the Coma galaxy cluster: First gamma-ray constraints ever on turbulent reacceleration. *Mon. Not. R. Astron. Soc.* **2017**, *472*, 1506–1525. [[CrossRef](#)]
65. Ackermann, M.; Ajello, M.; Albert, A.; Allafort, A.; Atwood, W.B.; Baldini, L.; Ballet, J.; Barbiellini, G.; Bastieri, D.; Bechtol, K.; et al. Search for Cosmic-Ray-induced Gamma-Ray Emission in Galaxy Clusters. *Astrophys. J.* **2014**, *787*, 18. [[CrossRef](#)]
66. Ackermann, M.; Ajello, M.; Albert, A.; Atwood, W.B.; Baldini, L.; Barbiellini, G.; Bastieri, D.; Bechtol, K.; Bellazzini, R.; Bissaldi, E.; et al. Search for Extended Gamma-Ray Emission from the Virgo Galaxy Cluster with FERMI-LAT. *Astrophys. J.* **2015**, *812*, 159. [[CrossRef](#)]
67. Ackermann, M.; Ajello, M.; Albert, A.; Atwood, W.B.; Baldini, L.; Ballet, J.; Barbiellini, G.; Bastieri, D.; Bechtol, K.; Bellazzini, R.; et al. Search for Gamma-Ray Emission from the Coma Cluster with Six Years of Fermi-LAT Data. *Astrophys. J.* **2016**, *819*, 149. [[CrossRef](#)]
68. Xi, S.Q.; Wang, X.Y.; Liang, Y.F.; Peng, F.K.; Yang, R.Z.; Liu, R.Y. Detection of gamma-ray emission from the Coma cluster with Fermi Large Area Telescope and tentative evidence for an extended spatial structure. *Phys. Rev. D* **2018**, *98*, 063006. [[CrossRef](#)]
69. Adam, R.; Goksu, H.; Brown, S.; Rudnick, L.; Ferrari, C.  $\gamma$ -ray detection toward the Coma cluster with Fermi-LAT: Implications for the cosmic ray content in the hadronic scenario. *Astron. Astrophys.* **2021**, *648*, A60. [[CrossRef](#)]
70. Baghmany, V.; Zargaryan, D.; Aharonian, F.; Yang, R.; Casanova, S.; Mackey, J. Detailed study of extended  $\gamma$ -ray morphology in the vicinity of the Coma cluster with Fermi Large Area Telescope. *Mon. Not. R. Astron. Soc.* **2022**, *516*, 562–571. [[CrossRef](#)]
71. Aleksić, J.; Alvarez, E.A.; Antonelli, L.A.; Antoranz, P.; Asensio, M.; Backes, M.; Barres de Almeida, U.; Barrio, J.A.; Bastieri, D.; Becerra González, J.; et al. Constraining cosmic rays and magnetic fields in the Perseus galaxy cluster with TeV observations by the MAGIC telescopes. *Astron. Astrophys.* **2012**, *541*, A99. [[CrossRef](#)]
72. Bonafede, A.; Feretti, L.; Murgia, M.; Govoni, F.; Giovannini, G.; Dallacasa, D.; Dolag, K.; Taylor, G.B. The Coma cluster magnetic field from Faraday rotation measures. *Astron. Astrophys.* **2010**, *513*, A30. [[CrossRef](#)]
73. Bonafede, A.; Vazza, F.; Brüggén, M.; Murgia, M.; Govoni, F.; Feretti, L.; Giovannini, G.; Ogrean, G. Measurements and simulation of Faraday rotation across the Coma radio relic. *Mon. Not. R. Astron. Soc.* **2013**, *433*, 3208–3226. [[CrossRef](#)]
74. Stuardi, C.; Bonafede, A.; Lovisari, L.; Domínguez-Fernández, P.; Vazza, F.; Brüggén, M.; van Weeren, R.J.; de Gasperin, F. The intracluster magnetic field in the double relic galaxy cluster Abell 2345. *Mon. Not. R. Astron. Soc.* **2021**, *502*, 2518–2535. [[CrossRef](#)]
75. Ferrière, K.; West, J.L.; Jaffe, T.R. The correct sense of Faraday rotation. *Mon. Not. R. Astron. Soc.* **2021**, *507*, 4968–4982. [[CrossRef](#)]
76. Lazarian, A.; Yuen, K.H. Gradients of Synchrotron Polarization: Tracing 3D Distribution of Magnetic Fields. *Astrophys. J.* **2018**, *865*, 59. [[CrossRef](#)]
77. Hurley-Walker, N.; Callingham, J.R.; Hancock, P.J.; Franzen, T.M.O.; Hindson, L.; Kapińska, A.D.; Morgan, J.; Offringa, A.R.; Wayth, R.B.; Wu, C.; et al. GaLactic and Extragalactic All-sky Murchison Widefield Array (GLEAM) survey—I. A low-frequency extragalactic catalogue. *Mon. Not. R. Astron. Soc.* **2017**, *464*, 1146–1167. [[CrossRef](#)]
78. Herrera Ruiz, N.; O’Sullivan, S.P.; Vacca, V.; Jelić, V.; Nikiel-Wroczyński, B.; Bourke, S.; Sabater, J.; Dettmar, R.J.; Heald, G.; Horellou, C.; et al. LOFAR Deep Fields: Probing a broader population of polarized radio galaxies in ELAIS-N1. *Astron. Astrophys.* **2021**, *648*, A12. [[CrossRef](#)]
79. Samui, S.; Subramanian, K.; Srianand, R. Efficient cold outflows driven by cosmic rays in high-redshift galaxies and their global effects on the IGM. *Mon. Not. R. Astron. Soc.* **2018**, *476*, 1680–1695. [[CrossRef](#)]
80. Federrath, C.; Klessen, R.S.; Iapichino, L.; Beattie, J.R. The sonic scale of interstellar turbulence. *Nat. Astron.* **2021**, *5*, 365–371. [[CrossRef](#)]
81. Schekochihin, A.; Cowley, S.; Maron, J.; Malyskin, L. Structure of small-scale magnetic fields in the kinematic dynamo theory. *Phys. Rev. E* **2001**, *65*, 016305. [[CrossRef](#)]

82. Schekochihin, A.A.; Cowley, S.C.; Taylor, S.F.; Maron, J.L.; McWilliams, J.C. Simulations of the Small-Scale Turbulent Dynamo. *Astrophys. J.* **2004**, *612*, 276–307. [[CrossRef](#)]
83. Kulsrud, R.M.; Ostriker, E.C. Plasma Physics for Astrophysics. *Phys. Today* **2006**, *59*, 58. [[CrossRef](#)]
84. Dolag, K.; Grasso, D.; Springel, V.; Tkachev, I. Constrained simulations of the magnetic field in the local Universe and the propagation of ultrahigh energy cosmic rays. *J. Cosmol. Astropart. Phys.* **2005**, *2005*, 009. [[CrossRef](#)]
85. Dolag, K.; Borgani, S.; Schindler, S.; Diaferio, A.; Bykov, A.M. Simulation Techniques for Cosmological Simulations. *Space Sci. Rev.* **2008**, *134*, 229–268. [[CrossRef](#)]
86. Iapichino, L.; Brüggén, M. Magnetic field amplification by shocks in galaxy clusters: application to radio relics. *Mon. Not. R. Astron. Soc.* **2012**, *423*, 2781–2788. [[CrossRef](#)]
87. Binney, J. Galaxy formation without primordial turbulence: Mechanisms for generating cosmic vorticity. *Mon. Not. R. Astron. Soc.* **1974**, *168*, 73–92. [[CrossRef](#)]
88. Lyutikov, M. Magnetic draping of merging cores and radio bubbles in clusters of galaxies. *Mon. Not. R. Astron. Soc.* **2006**, *373*, 73–78. [[CrossRef](#)]
89. Dennison, B. Formation of radio halos in clusters of galaxies from cosmic-ray protons. *Astrophys. J.* **1980**, *239*, L93–L96. [[CrossRef](#)]
90. Pfrommer, C.; Enßlin, T.A.; Springel, V. Simulating cosmic rays in clusters of galaxies—II. A unified scheme for radio haloes and relics with predictions of the  $\gamma$ -ray emission. *Mon. Not. R. Astron. Soc.* **2008**, *385*, 1211–1241. [[CrossRef](#)]
91. Enßlin, T.; Pfrommer, C.; Miniati, F.; Subramanian, K. Cosmic ray transport in galaxy clusters: Implications for radio halos, gamma-ray signatures, and cool core heating. *Astron. Astrophys.* **2011**, *527*, A99. [[CrossRef](#)]
92. Sreekumar, P.; Bertsch, D.L.; Dingus, B.L.; Esposito, J.A.; Fichtel, C.E.; Fierro, J.; Hartman, R.C.; Hunter, S.D.; Kanbach, G.; Kniffen, D.A.; et al. EGRET Observations of the North Galactic Pole Region. *Astrophys. J.* **1996**, *464*, 628. [[CrossRef](#)]
93. Reimer, O.; Pohl, M.; Sreekumar, P.; Mattox, J.R. EGRET Upper Limits on the High-Energy Gamma-Ray Emission of Galaxy Clusters. *Astrophys. J.* **2003**, *588*, 155–164. [[CrossRef](#)]
94. Huber, B.; Tchernin, C.; Eckert, D.; Farnier, C.; Manalaysay, A.; Straumann, U.; Walter, R. Probing the cosmic-ray content of galaxy clusters by stacking Fermi-LAT count maps. *Astron. Astrophys.* **2013**, *560*, A64. [[CrossRef](#)]
95. Zandanel, F.; Ando, S. Constraints on diffuse gamma-ray emission from structure formation processes in the Coma cluster. *Mon. Not. R. Astron. Soc.* **2014**, *440*, 663–671. [[CrossRef](#)]
96. Aharonian, F.; Akhperjanian, A.G.; Anton, G.; Barres de Almeida, U.; Bazer-Bachi, A.R.; Becherini, Y.; Behera, B.; Bernlöhr, K.; Boisson, C.; Bochow, A.; et al. Very high energy gamma-ray observations of the galaxy clusters Abell 496 and Abell 85 with HESS. *Astron. Astrophys.* **2009**, *495*, 27–35. [[CrossRef](#)]
97. Aleksić, J.; Antonelli, L.A.; Antoranz, P.; Backes, M.; Baixeras, C.; Balestra, S.; Barrio, J.A.; Bastieri, D.; Becerra González, J.; Bednarek, W.; et al. MAGIC Gamma-ray Telescope Observation of the Perseus Cluster of Galaxies: Implications for Cosmic Rays, Dark Matter, and NGC 1275. *Astrophys. J.* **2010**, *710*, 634–647. [[CrossRef](#)]
98. Arlen, T.; Aune, T.; Beilicke, M.; Benbow, W.; Bouvier, A.; Buckley, J.H.; Bugaev, V.; Byrum, K.; Cannon, A.; Cesarini, A.; et al. Constraints on Cosmic Rays, Magnetic Fields, and Dark Matter from Gamma-Ray Observations of the Coma Cluster of Galaxies with VERITAS and Fermi. *Astrophys. J.* **2012**, *757*, 123. [[CrossRef](#)]
99. Ahnen, M.L.; Ansoldi, S.; Antonelli, L.A.; Antoranz, P.; Babic, A.; Banerjee, B.; Bangale, P.; Barres de Almeida, U.; Barrio, J.A.; Becerra González, J.; et al. Deep observation of the NGC 1275 region with MAGIC: Search of diffuse  $\gamma$ -ray emission from cosmic rays in the Perseus cluster. *Astron. Astrophys.* **2016**, *589*, A33. [[CrossRef](#)]
100. Brunetti, G.; Blasi, P.; Reimer, O.; Rudnick, L.; Bonafede, A.; Brown, S. Probing the origin of giant radio haloes through radio and  $\gamma$ -ray data: The case of the Coma cluster. *Mon. Not. R. Astron. Soc.* **2012**, *426*, 956–968. [[CrossRef](#)]
101. Bruno, L.; Rajpurohit, K.; Brunetti, G.; Gastaldello, F.; Botteon, A.; Ignesti, A.; Bonafede, A.; Dallacasa, D.; Cassano, R.; van Weeren, R.J.; et al. The LOFAR and JVLA view of the distant steep spectrum radio halo in MACS J1149.5+2223. *Astron. Astrophys.* **2021**, *650*, A44. [[CrossRef](#)]
102. Fisk, L.A. The acceleration of energetic particles in the interplanetary medium by transit time damping. *J. Geophys. Res.* **1976**, *81*, 4633. [[CrossRef](#)]
103. Schlickeiser, R.; Miller, J.A. Quasi-linear Theory of Cosmic-Ray Transport and Acceleration: The Role of Oblique Magnetohydrodynamic Waves and Transit-Time Damping. *Astrophys. J.* **1998**, *492*, 352–378. [[CrossRef](#)]
104. Pilipp, W.; Völk, H.J. Analysis of electromagnetic instabilities parallel to the magnetic field. *J. Plasma Phys.* **1971**, *6*, 1–17. [[CrossRef](#)]
105. Yan, H.; Lazarian, A. Cosmic-Ray Scattering and Streaming in Compressible Magnetohydrodynamic Turbulence. *Astrophys. J.* **2004**, *614*, 757–769. [[CrossRef](#)]
106. Lazarian, A.; Beresnyak, A. Cosmic ray scattering in compressible turbulence. *Mon. Not. R. Astron. Soc.* **2006**, *373*, 1195–1202. [[CrossRef](#)]
107. Eilek, J.A. Particle reacceleration in radio galaxies. *Astrophys. J.* **1979**, *230*, 373–385. [[CrossRef](#)]
108. Porter, D.H.; Jones, T.W.; Ryu, D. Vorticity, Shocks, and Magnetic Fields in Subsonic, ICM-like Turbulence. *Astrophys. J.* **2015**, *810*, 93. [[CrossRef](#)]
109. Brunetti, G.; Lazarian, A. Stochastic reacceleration of relativistic electrons by turbulent reconnection: A mechanism for cluster-scale radio emission? *Mon. Not. R. Astron. Soc.* **2016**, *458*, 2584–2595. [[CrossRef](#)]

110. Cassano, R.; Etti, S.; Giacintucci, S.; Brunetti, G.; Markevitch, M.; Venturi, T.; Gitti, M. On the Connection Between Giant Radio Halos and Cluster Mergers. *Astrophys. J.* **2010**, *721*, L82–L85. [[CrossRef](#)]
111. Cuciti, V.; Cassano, R.; Brunetti, G.; Dallacasa, D.; de Gasperin, F.; Etti, S.; Giacintucci, S.; Kale, R.; Pratt, G.W.; van Weeren, R.J.; et al. Radio halos in a mass-selected sample of 75 galaxy clusters. II. Statistical analysis. *Astron. Astrophys.* **2021**, *647*, A51. [[CrossRef](#)]
112. Cuciti, V.; Cassano, R.; Brunetti, G.; Dallacasa, D.; van Weeren, R.J.; Giacintucci, S.; Bonafede, A.; de Gasperin, F.; Etti, S.; Kale, R.; et al. Radio halos in a mass-selected sample of 75 galaxy clusters. I. Sample selection and data analysis. *Astron. Astrophys.* **2021**, *647*, A50. [[CrossRef](#)]
113. Wilber, A.; Brügger, M.; Bonafede, A.; Savini, F.; Shimwell, T.; van Weeren, R.J.; Rafferty, D.; Mechev, A.P.; Intema, H.; Andrade-Santos, F.; et al. LOFAR discovery of an ultra-steep radio halo and giant head-tail radio galaxy in Abell 1132. *Mon. Not. R. Astron. Soc.* **2018**, *473*, 3536–3546. [[CrossRef](#)]
114. Rajpurohit, K.; Brunetti, G.; Bonafede, A.; van Weeren, R.J.; Botteon, A.; Vazza, F.; Hoeft, M.; Riseley, C.J.; Bonnassieux, E.; Brienza, M.; et al. Physical insights from the spectrum of the radio halo in MACS J0717.5+3745. *Astron. Astrophys.* **2021**, *646*, A135. [[CrossRef](#)]
115. Vacca, V.; Govoni, F.; Perley, R.A.; Murgia, M.; Carretti, E.; Loi, F.; Feretti, L.; Giovannini, G. Spectral Index of the Filaments in the Abell 523 Radio Halo. *Galaxies* **2021**, *9*, 112. [[CrossRef](#)]
116. Di Gennaro, G.; van Weeren, R.J.; Cassano, R.; Brunetti, G.; Brügger, M.; Hoeft, M.; Osinga, E.; Botteon, A.; Cuciti, V.; de Gasperin, F.; et al. A LOFAR-uGMRT spectral index study of distant radio halos. *Astron. Astrophys.* **2021**, *654*, A166. [[CrossRef](#)]
117. Duchesne, S.W.; Johnston-Hollitt, M.; Wilber, A.G. MWA and ASKAP observations of atypical radio-halo-hosting galaxy clusters: Abell 141 and Abell 3404. *Publ. Astron. Soc. Aust.* **2021**, *38*, e031. [[CrossRef](#)]
118. Duchesne, S.W.; Johnston-Hollitt, M.; Bartalucci, I. Low-frequency integrated radio spectra of diffuse, steep-spectrum sources in galaxy clusters: Palaeontology with the MWA and ASKAP. *Publ. Astron. Soc. Aust.* **2021**, *38*, e053. [[CrossRef](#)]
119. Botteon, A.; Brunetti, G.; van Weeren, R.J.; Shimwell, T.W.; Pizzo, R.F.; Cassano, R.; Iacobelli, M.; Gastaldello, F.; Birzan, L.; Bonafede, A.; et al. The Beautiful Mess in Abell 2255. *Astrophys. J.* **2020**, *897*, 93. [[CrossRef](#)]
120. Bonafede, A.; Brunetti, G.; Rudnick, L.; Vazza, F.; Bourdin, H.; Giovannini, G.; Shimwell, T.W.; Zhang, X.; Mazzotta, P.; Simionescu, A.; et al. The Coma Cluster at LOFAR Frequencies. II. The Halo, Relic, and a New Accretion Relic. *Astrophys. J.* **2022**, *933*, 218. [[CrossRef](#)]
121. Cassano, R.; Etti, S.; Brunetti, G.; Giacintucci, S.; Pratt, G.W.; Venturi, T.; Kale, R.; Dolag, K.; Markevitch, M. Revisiting Scaling Relations for Giant Radio Halos in Galaxy Clusters. *Astrophys. J.* **2013**, *777*, 141. [[CrossRef](#)]
122. Cassano, R.; Brunetti, G.; Setti, G. Statistics of giant radio haloes from electron reacceleration models. *Mon. Not. R. Astron. Soc.* **2006**, *369*, 1577–1595. [[CrossRef](#)]
123. Angelinelli, M.; Vazza, F.; Giocoli, C.; Etti, S.; Jones, T.W.; Brunetti, G.; Brügger, M.; Eckert, D. Turbulent pressure support and hydrostatic mass bias in the intracluster medium. *Mon. Not. R. Astron. Soc.* **2020**, *495*, 864–885. [[CrossRef](#)]
124. Simonte, M.; Vazza, F.; Brighenti, F.; Brügger, M.; Jones, T.W.; Angelinelli, M. Exploring the relation between turbulent velocity and density fluctuations in the stratified intracluster medium. *Astron. Astrophys.* **2022**, *658*, A149. [[CrossRef](#)]
125. Sanders, J.S.; Biffi, V.; Brügger, M.; Bulbul, E.; Dennerl, K.; Dolag, K.; Erben, T.; Freyberg, M.; Gatuzz, E.; Ghirardini, V.; et al. Studying the merging cluster Abell 3266 with eROSITA. *Astron. Astrophys.* **2022**, *661*, A36. [[CrossRef](#)]
126. de Vries, M.; Mantz, A.B.; Allen, S.W.; Morris, R.G.; Zhuravleva, I.; Canning, R.E.A.; Ehlert, S.R.; Ogorzałek, A.; Simionescu, A.; Werner, N. Chandra measurements of gas homogeneity and turbulence at intermediate radii in the Perseus Cluster. *Mon. Not. R. Astron. Soc.* **2023**, *518*, 2954–2970. [[CrossRef](#)]
127. Dupourqué, S.; Clerc, N.; Pointecouteau, E.; Eckert, D.; Etti, S.; Vazza, F. Investigating the turbulent hot gas in X-COP galaxy clusters. *arXiv* **2023**, arXiv:2303.15102. <https://doi.org/10.48550/arXiv.2303.15102>.
128. Zhuravleva, I.; Chen, M.C.; Churazov, E.; Schekochihin, A.A.; Zhang, C.; Nagai, D. Indirect measurements of gas velocities in galaxy clusters: Effects of ellipticity and cluster dynamic state. *Mon. Not. R. Astron. Soc.* **2023**, *520*, 5157–5172. [[CrossRef](#)]
129. Riseley, C.J.; Bonnassieux, E.; Vernstrom, T.; Galvin, T.J.; Chokshi, A.; Botteon, A.; Rajpurohit, K.; Duchesne, S.W.; Bonafede, A.; Rudnick, L.; et al. Radio fossils, relics, and haloes in Abell 3266: Cluster archaeology with ASKAP-EMU and the ATCA. *Mon. Not. R. Astron. Soc.* **2022**, *515*, 1871–1896. [[CrossRef](#)]
130. Hoang, D.N.; Zhang, X.; Stuardi, C.; Shimwell, T.W.; Bonafede, A.; Brügger, M.; Brunetti, G.; Botteon, A.; Cassano, R.; de Gasperin, F.; et al. A 3.5 Mpc long radio relic in the galaxy cluster CIG 0217+70. *Astron. Astrophys.* **2021**, *656*, A154. [[CrossRef](#)]
131. Dolag, K.; Enßlin, T.A. Radio halos of galaxy clusters from hadronic secondary electron injection in realistic magnetic field configurations. *Astron. Astrophys.* **2000**, *362*, 151–157. [[CrossRef](#)]
132. Govoni, F.; Feretti, L.; Giovannini, G.; Böhringer, H.; Reiprich, T.H.; Murgia, M. Radio and X-ray diffuse emission in six clusters of galaxies. *Astron. Astrophys.* **2001**, *376*, 803–819. [[CrossRef](#)]
133. Storm, E.; Jeltama, T.E.; Rudnick, L. A radio and X-ray study of the merging cluster A2319. *Mon. Not. R. Astron. Soc.* **2015**, *448*, 2495–2503. [[CrossRef](#)]
134. Rajpurohit, K.; Osinga, E.; Brienza, M.; Botteon, A.; Brunetti, G.; Forman, W.R.; Riseley, C.J.; Vazza, F.; Bonafede, A.; van Weeren, R.J.; et al. Deep low-frequency radio observations of Abell 2256. II. The ultra-steep spectrum radio halo. *Astron. Astrophys.* **2023**, *669*, A1. [[CrossRef](#)]

135. Cuciti, V.; de Gasperin, F.; Brügggen, M.; Vazza, F.; Brunetti, G.; Shimwell, T.W.; Edler, H.W.; van Weeren, R.J.; Botteon, A.; Cassano, R.; et al. Galaxy clusters enveloped by vast volumes of relativistic electrons. *Nature* **2022**, *609*, 911–914. [[CrossRef](#)]
136. Botteon, A.; van Weeren, R.J.; Brunetti, G.; Vazza, F.; Shimwell, T.W.; Brügggen, M.; Röttgering, H.J.A.; de Gasperin, F.; Akamatsu, H.; Bonafede, A.; et al. Magnetic fields and relativistic electrons fill entire galaxy cluster. *Sci. Adv.* **2022**, *8*, eabq7623. [[CrossRef](#)] [[PubMed](#)]
137. Govoni, F.; Murgia, M.; Xu, H.; Li, H.; Norman, M.L.; Feretti, L.; Giovannini, G.; Vacca, V. Polarization of cluster radio halos with upcoming radio interferometers. *Astron. Astrophys.* **2013**, *554*, A102. [[CrossRef](#)]
138. Loi, F.; Murgia, M.; Govoni, F.; Vacca, V.; Prandoni, I.; Li, H.; Feretti, L.; Giovannini, G. Simulations of the Polarized Sky for the SKA: How to Constrain Intracluster Magnetic Fields. *Galaxies* **2018**, *6*, 133. [[CrossRef](#)]
139. Loi, F.; Murgia, M.; Govoni, F.; Vacca, V.; Bonafede, A.; Ferrari, C.; Prandoni, I.; Feretti, L.; Giovannini, G.; Li, H. Rotation measure synthesis applied to synthetic SKA images of galaxy clusters. *Mon. Not. R. Astron. Soc.* **2019**, *490*, 4841–4857. [[CrossRef](#)]
140. Basu, A.; Sur, S. Properties of Polarized Synchrotron Emission from Fluctuation Dynamo Action—II. Effects of Turbulence Driving in the ICM and Beam Smoothing. *Galaxies* **2021**, *9*, 62. [[CrossRef](#)]
141. Govoni, F.; Murgia, M.; Feretti, L.; Giovannini, G.; Dallacasa, D.; Taylor, G.B. A2255: The first detection of filamentary polarized emission in a radio halo. *Astron. Astrophys.* **2005**, *430*, L5–L8. [[CrossRef](#)]
142. Bonafede, A.; Feretti, L.; Giovannini, G.; Govoni, F.; Murgia, M.; Taylor, G.B.; Ebeling, H.; Allen, S.; Gentile, G.; Pihlström, Y. Revealing the magnetic field in a distant galaxy cluster: Discovery of the complex radio emission from MACS J0717.5 +3745. *Astron. Astrophys.* **2009**, *503*, 707–720. [[CrossRef](#)]
143. Girardi, M.; Boschini, W.; Gastaldello, F.; Giovannini, G.; Govoni, F.; Murgia, M.; Barrera, R.; Ettori, S.; Trasatti, M.; Vacca, V. A multiwavelength view of the galaxy cluster Abell 523 and its peculiar diffuse radio source. *Mon. Not. R. Astron. Soc.* **2016**, *456*, 2829–2847. [[CrossRef](#)]
144. Rajpurohit, K.; Hoeft, M.; Wittor, D.; van Weeren, R.J.; Vazza, F.; Rudnick, L.; Rajpurohit, S.; Forman, W.R.; Riseley, C.J.; Brienza, M.; et al. Turbulent magnetic fields in the merging galaxy cluster MACS J0717.5+3745. *Astron. Astrophys.* **2022**, *657*, A2. [[CrossRef](#)]
145. Sur, S.; Basu, A.; Subramanian, K. Properties of polarized synchrotron emission from fluctuation-dynamo action—I. Application to galaxy clusters. *Mon. Not. R. Astron. Soc.* **2021**, *501*, 3332–3349. [[CrossRef](#)]
146. Di Gennaro, G.; van Weeren, R.J.; Brunetti, G.; Cassano, R.; Brügggen, M.; Hoeft, M.; Shimwell, T.W.; Röttgering, H.J.A.; Bonafede, A.; Botteon, A.; et al. Fast magnetic field amplification in distant galaxy clusters. *Nat. Astron.* **2021**, *5*, 268–275. [[CrossRef](#)]
147. Giacintucci, S.; Markevitch, M.; Venturi, T.; Clarke, T.E.; Cassano, R.; Mazzotta, P. New Detections of Radio Minihalos in Cool Cores of Galaxy Clusters. *Astrophys. J.* **2014**, *781*, 9. [[CrossRef](#)]
148. Giacintucci, S.; Markevitch, M.; Brunetti, G.; ZuHone, J.A.; Venturi, T.; Mazzotta, P.; Bourdin, H. Mapping the Particle Acceleration in the Cool Core of the Galaxy Cluster RX J1720.1+2638. *Astrophys. J.* **2014**, *795*, 73. [[CrossRef](#)]
149. Giacintucci, S.; Markevitch, M.; Cassano, R.; Venturi, T.; Clarke, T.E.; Brunetti, G. Occurrence of Radio Minihalos in a Mass-limited Sample of Galaxy Clusters. *Astrophys. J.* **2017**, *841*, 71. [[CrossRef](#)]
150. ZuHone, J.A.; Brunetti, G.; Giacintucci, S.; Markevitch, M. Testing Secondary Models for the Origin of Radio Mini-Halos in Galaxy Clusters. *Astrophys. J.* **2015**, *801*, 146. [[CrossRef](#)]
151. Riseley, C.J.; Rajpurohit, K.; Loi, F.; Botteon, A.; Timmerman, R.; Biava, N.; Bonafede, A.; Bonnassieux, E.; Brunetti, G.; Enßlin, T.; et al. A MeerKAT-meets-LOFAR study of MS 1455.0 + 2232: A 590 kiloparsec ‘mini’-halo in a sloshing cool-core cluster. *Mon. Not. R. Astron. Soc.* **2022**, *512*, 4210–4230. [[CrossRef](#)]
152. Mazzotta, P.; Markevitch, M.; Vikhlinin, A.; Forman, W.R.; David, L.P.; van Speybroeck, L. Chandra Observation of RX J1720.1+2638: A Nearly Relaxed Cluster with a Fast-moving Core? *Astrophys. J.* **2001**, *555*, 205–214. [[CrossRef](#)]
153. Mazzotta, P.; Giacintucci, S. Do Radio Core-Halos and Cold Fronts in Non-Major-Merging Clusters Originate from the Same Gas Sloshing? *Astrophys. J.* **2008**, *675*, L9. [[CrossRef](#)]
154. Rossetti, M.; Eckert, D.; De Grandi, S.; Gastaldello, F.; Ghizzardi, S.; Roediger, E.; Molendi, S. Abell 2142 at large scales: An extreme case for sloshing? *Astron. Astrophys.* **2013**, *556*, A44. [[CrossRef](#)]
155. Savini, F.; Bonafede, A.; Brügggen, M.; van Weeren, R.; Brunetti, G.; Intema, H.; Botteon, A.; Shimwell, T.; Wilber, A.; Rafferty, D.; et al. First evidence of diffuse ultra-steep-spectrum radio emission surrounding the cool core of a cluster. *Mon. Not. R. Astron. Soc.* **2018**, *478*, 2234–2242. [[CrossRef](#)]
156. Fujita, Y.; Kohri, K.; Yamazaki, R.; Kino, M. Nonthermal Emission Associated with Strong AGN Outbursts at the Centers of Galaxy Clusters. *Astrophys. J.* **2007**, *663*, L61–L64. [[CrossRef](#)]
157. Bravi, L.; Gitti, M.; Brunetti, G. Do radio mini-halos and gas heating in cool-core clusters have a common origin? *Mon. Not. R. Astron. Soc.* **2016**, *455*, L41–L45. [[CrossRef](#)]
158. Richard-Laferrrière, A.; Hlavacek-Larrondo, J.; Nemmen, R.S.; Rhea, C.L.; Taylor, G.B.; Prasow-Émond, M.; Gendron-Marsolais, M.; Latulippe, M.; Edge, A.C.; Fabian, A.C.; et al. On the relation between mini-halos and AGN feedback in clusters of galaxies. *Mon. Not. R. Astron. Soc.* **2020**, *499*, 2934–2958. [[CrossRef](#)]
159. Ignesti, A.; Brunetti, G.; Gitti, M.; Giacintucci, S. Radio and X-ray connection in radio mini-halos: Implications for hadronic models. *Astron. Astrophys.* **2020**, *640*, A37. [[CrossRef](#)]
160. Skillman, S.W.; Hallman, E.J.; O’Shea, B.W.; Burns, J.O. Cosmological Shockwaves as Plasma Physics Laboratories: Radio Relics and Electron Acceleration. In *Bulletin of the American Astronomical Society*; American Astronomical Society: Washington, DC, USA, 2010; Volume 42, p. 389.

161. Kang, H.; Ryu, D.; Jones, T.W. Diffusive Shock Acceleration Simulations of Radio Relics. *Astrophys. J.* **2012**, *756*, 97. [[CrossRef](#)]
162. Skillman, S.W.; Xu, H.; Hallman, E.J.; O'Shea, B.W.; Burns, J.O.; Li, H.; Collins, D.C.; Norman, M.L. Cosmological Magnetohydrodynamic Simulations of Galaxy Cluster Radio Relics: Insights and Warnings for Observations. *Astrophys. J.* **2013**, *765*, 21. [[CrossRef](#)]
163. Vazza, F.; Brüggen, M. Do radio relics challenge diffusive shock acceleration? *Mon. Not. R. Astron. Soc.* **2014**, *437*, 2291–2296. [[CrossRef](#)]
164. Trasatti, M.; Akamatsu, H.; Lovisari, L.; Klein, U.; Bonafede, A.; Brüggen, M.; Dallacasa, D.; Clarke, T. The radio relic in Abell 2256: Overall spectrum and implications for electron acceleration. *Astron. Astrophys.* **2015**, *575*, A45. [[CrossRef](#)]
165. Locatelli, N.T.; Rajpurohit, K.; Vazza, F.; Gastaldello, F.; Dallacasa, D.; Bonafede, A.; Rossetti, M.; Stuardi, C.; Bonassieux, E.; Brunetti, G.; et al. Discovering the most elusive radio relic in the sky: Diffuse shock acceleration caught in the act? *Mon. Not. R. Astron. Soc.* **2020**, *496*, L48–L53. [[CrossRef](#)]
166. Brüggen, M.; Vazza, F. Analytical model for cluster radio relics. *Mon. Not. R. Astron. Soc.* **2020**, *493*, 2306–2317. [[CrossRef](#)]
167. Fermi, E. On the Origin of the Cosmic Radiation. *Phys. Rev.* **1949**, *75*, 1169–1174. [[CrossRef](#)]
168. Blandford, R.D.; Ostriker, J.P. Particle acceleration by astrophysical shocks. *Astrophys. J.* **1978**, *221*, L29–L32. [[CrossRef](#)]
169. Drury, L.O. An introduction to the theory of diffusive shock acceleration of energetic particles in tenuous plasmas. *Rep. Prog. Phys.* **1983**, *46*, 973–1027. [[CrossRef](#)]
170. Loi, F.; Murgia, M.; Vacca, V.; Govoni, F.; Melis, A.; Wittor, D.; Kierdorf, M.; Bonafede, A.; Boschin, W.; Brienza, M.; et al. Spectropolarimetric observations of the CIZA J2242.8+5301 northern radio relic: No evidence of high-frequency steepening. *Mon. Not. R. Astron. Soc.* **2020**, *498*, 1628–1637. [[CrossRef](#)]
171. Rajpurohit, K.; Wittor, D.; van Weeren, R.J.; Vazza, F.; Hoeft, M.; Rudnick, L.; Locatelli, N.; Eilek, J.; Forman, W.R.; Bonafede, A.; et al. Understanding the radio relic emission in the galaxy cluster MACS J0717.5+3745: Spectral analysis. *Astron. Astrophys.* **2021**, *646*, A56. [[CrossRef](#)]
172. Rajpurohit, K.; Hoeft, M.; Vazza, F.; Rudnick, L.; van Weeren, R.J.; Wittor, D.; Drabent, A.; Brienza, M.; Bonassieux, E.; Locatelli, N.; et al. New mysteries and challenges from the Toothbrush relic: Wideband observations from 550 MHz to 8 GHz. *Astron. Astrophys.* **2020**, *636*, A30. [[CrossRef](#)]
173. Rajpurohit, K.; Vazza, F.; Hoeft, M.; Loi, F.; Beck, R.; Vacca, V.; Kierdorf, M.; van Weeren, R.J.; Wittor, D.; Govoni, F.; et al. A perfect power-law spectrum even at the highest frequencies: The Toothbrush relic. *Astron. Astrophys.* **2020**, *642*, L13. [[CrossRef](#)]
174. Schellenberger, G.; Giacintucci, S.; Lovisari, L.; O'Sullivan, E.; Vrtilik, J.; David, L.P.; Melin, J.B.; Lal, D.V.; Ettori, S.; Kolokythas, K.; et al. The Unusually Weak and Exceptionally Steep Radio Relic in A2108. *Astrophys. J.* **2022**, *925*, 91. [[CrossRef](#)]
175. Stuardi, C.; Bonafede, A.; Wittor, D.; Vazza, F.; Botteon, A.; Locatelli, N.; Dallacasa, D.; Golovich, N.; Hoeft, M.; van Weeren, R.J.; et al. Particle re-acceleration and Faraday-complex structures in the RXC J1314.4-2515 galaxy cluster. *Mon. Not. R. Astron. Soc.* **2019**, *489*, 3905–3926. [[CrossRef](#)]
176. Di Gennaro, G.; van Weeren, R.J.; Hoeft, M.; Kang, H.; Ryu, D.; Rudnick, L.; Forman, W.; Röttgering, H.J.A.; Brüggen, M.; Dawson, W.A.; et al. Deep Very Large Array Observations of the Merging Cluster CIZA J2242.8+5301: Continuum and Spectral Imaging. *Astrophys. J.* **2018**, *865*, 24. [[CrossRef](#)]
177. Jones, A.; de Gasperin, F.; Cuciti, V.; Hoang, D.N.; Botteon, A.; Brüggen, M.; Brunetti, G.; Finner, K.; Forman, W.R.; Jones, C.; et al. Radio relics in PSZ2 G096.88+24.18: A connection with pre-existing plasma. *Mon. Not. R. Astron. Soc.* **2021**, *505*, 4762–4774. [[CrossRef](#)]
178. Kang, H.; Ryu, D. Diffusive Shock Acceleration at Cosmological Shock Waves. *Astrophys. J.* **2013**, *764*, 95. [[CrossRef](#)]
179. Kang, H. Shock Acceleration Model with Postshock Turbulence for Giant Radio Relics. *J. Korean Astron. Soc.* **2017**, *50*, 93–103. [[CrossRef](#)]
180. Kang, H.; Ryu, D. Effects of Alfvénic Drift on Diffusive Shock Acceleration at Weak Cluster Shocks. *Astrophys. J.* **2018**, *856*, 33. [[CrossRef](#)]
181. Kang, H. Semi-Analytic Models for Electron Acceleration in Weak ICM Shocks. *J. Korean Astron. Soc.* **2020**, *53*, 59–67.
182. Caprioli, D.; Spitkovsky, A. Simulations of Ion Acceleration at Non-relativistic Shocks. II. Magnetic Field Amplification. *Astrophys. J.* **2014**, *794*, 46. [[CrossRef](#)]
183. Caprioli, D.; Zhang, H.; Spitkovsky, A. Diffusive shock re-acceleration. *J. Plasma Phys.* **2018**, *84*, 715840301. [[CrossRef](#)]
184. Caprioli, D.; Haggerty, C.C.; Blasi, P. Kinetic Simulations of Cosmic-Ray-modified Shocks. II. Particle Spectra. *Astrophys. J.* **2020**, *905*, 2. [[CrossRef](#)]
185. Guo, X.; Sironi, L.; Narayan, R. Non-thermal Electron Acceleration in Low Mach Number Collisionless Shocks. I. Particle Energy Spectra and Acceleration Mechanism. *Astrophys. J.* **2014**, *794*, 153. [[CrossRef](#)]
186. Guo, X.; Sironi, L.; Narayan, R. Non-thermal Electron Acceleration in Low Mach Number Collisionless Shocks. II. Firehose-mediated Fermi Acceleration and its Dependence on Pre-shock Conditions. *Astrophys. J.* **2014**, *797*, 47. [[CrossRef](#)]
187. Pais, M.; Pfrommer, C.; Ehlert, K.; Pakmor, R. The effect of cosmic ray acceleration on supernova blast wave dynamics. *Mon. Not. R. Astron. Soc.* **2018**, *478*, 5278–5295. [[CrossRef](#)]
188. Dubois, Y.; Commerçon, B.; Marcowith, A.; Brahim, L. Shock-accelerated cosmic rays and streaming instability in the adaptive mesh refinement code Ramses. *Astron. Astrophys.* **2019**, *631*, A121. [[CrossRef](#)]
189. Botteon, A.; Brunetti, G.; Ryu, D.; Roh, S. Shock acceleration efficiency in radio relics. *Astron. Astrophys.* **2020**, *634*, A64. [[CrossRef](#)]

190. Bonafede, A.; Intema, H.T.; Brügggen, M.; Girardi, M.; Nonino, M.; Kantharia, N.; van Weeren, R.J.; Röttgering, H.J.A. Evidence for Particle Re-acceleration in the Radio Relic in the Galaxy Cluster PLCKG287.0+32.9. *Astrophys. J.* **2014**, *785*, 1. [[CrossRef](#)]
191. van Weeren, R.J.; Andrade-Santos, F.; Dawson, W.A.; Golovich, N.; Lal, D.V.; Kang, H.; Ryu, D.; Brügggen, M.; Ogorean, G.A.; Forman, W.R.; et al. The case for electron re-acceleration at galaxy cluster shocks. *Nat. Astron.* **2017**, *1*, 0005. [[CrossRef](#)]
192. Inchingolo, G.; Wittor, D.; Rajpurohit, K.; Vazza, F. Radio relics radio emission from multishock scenario. *Mon. Not. R. Astron. Soc.* **2022**, *509*, 1160–1174. [[CrossRef](#)]
193. ZuHone, J.A.; Markevitch, M.; Weinberger, R.; Nulsen, P.; Ehlert, K. How Merger-driven Gas Motions in Galaxy Clusters Can Turn AGN Bubbles into Radio Relics. *Astrophys. J.* **2021**, *914*, 73. [[CrossRef](#)]
194. ZuHone, J.; Ehlert, K.; Weinberger, R.; Pfrommer, C. Turning AGN Bubbles into Radio Relics with Sloshing: Modeling CR Transport with Realistic Physics. *Galaxies* **2021**, *9*, 91. [[CrossRef](#)]
195. Lee, W.; James Jee, M.; Finner, K.; HyeonHan, K.; Kale, R.; Yoon, H.; Forman, W.; Kraft, R.; Jones, C.; Chung, A. Discovery of a Double Radio Relic in ZwCl1447.2+2619: A Rare Testbed for Shock-acceleration Models with a Peculiar Surface-brightness Ratio. *Astrophys. J.* **2022**, *924*, 18. [[CrossRef](#)]
196. Matsukiyo, S.; Ohira, Y.; Yamazaki, R.; Umeda, T. Relativistic Electron Shock Drift Acceleration in Low Mach Number Galaxy Cluster Shocks. *Astrophys. J.* **2011**, *742*, 47. [[CrossRef](#)]
197. Akamatsu, H.; Kawahara, H. Systematic X-ray Analysis of Radio Relic Clusters with Suzaku. *Publ. Astron. Soc. Jpn.* **2013**, *65*, 16. [[CrossRef](#)]
198. Eckert, D.; Jauzac, M.; Vazza, F.; Owers, M.S.; Kneib, J.P.; Tchernin, C.; Intema, H.; Knowles, K. A shock front at the radio relic of Abell 2744. *Mon. Not. R. Astron. Soc.* **2016**, *461*, 1302–1307. [[CrossRef](#)]
199. van Weeren, R.J.; Brunetti, G.; Brügggen, M.; Andrade-Santos, F.; Ogorean, G.A.; Williams, W.L.; Röttgering, H.J.A.; Dawson, W.A.; Forman, W.R.; de Gasperin, F.; et al. LOFAR, VLA, and Chandra Observations of the Toothbrush Galaxy Cluster. *Astrophys. J.* **2016**, *818*, 204. [[CrossRef](#)]
200. Hoang, D.N.; Shimwell, T.W.; van Weeren, R.J.; Intema, H.T.; Röttgering, H.J.A.; Andrade-Santos, F.; Akamatsu, H.; Bonafede, A.; Brunetti, G.; Dawson, W.A.; et al. Radio observations of the double-relic galaxy cluster Abell 1240. *Mon. Not. R. Astron. Soc.* **2018**, *478*, 2218–2233. [[CrossRef](#)]
201. Markevitch, M.; Govoni, F.; Brunetti, G.; Jerius, D. Bow Shock and Radio Halo in the Merging Cluster A520. *Astrophys. J.* **2005**, *627*, 733–738. [[CrossRef](#)]
202. Hong, S.E.; Kang, H.; Ryu, D. Radio and X-Ray Shocks in Clusters of Galaxies. *Astrophys. J.* **2015**, *812*, 49. [[CrossRef](#)]
203. Kang, H.; Ryu, D. Curved Radio Spectra of Weak Cluster Shocks. *Astrophys. J.* **2015**, *809*, 186. [[CrossRef](#)]
204. Stroe, A.; Shimwell, T.; Rumsey, C.; van Weeren, R.; Kierdorf, M.; Donnert, J.; Jones, T.W.; Röttgering, H.J.A.; Hoeft, M.; Rodríguez-Gonzálvez, C.; et al. The widest frequency radio relic spectra: Observations from 150 MHz to 30 GHz. *Mon. Not. R. Astron. Soc.* **2016**, *455*, 2402–2416. [[CrossRef](#)]
205. Akamatsu, H.; Mizuno, M.; Ota, N.; Zhang, Y.Y.; van Weeren, R.J.; Kawahara, H.; Fukazawa, Y.; Kaastra, J.S.; Kawaharada, M.; Nakazawa, K.; et al. Suzaku observations of the merging galaxy cluster Abell 2255: The northeast radio relic. *Astron. Astrophys.* **2017**, *600*, A100. [[CrossRef](#)]
206. Hoang, D.N.; Shimwell, T.W.; Stroe, A.; Akamatsu, H.; Brunetti, G.; Donnert, J.M.F.; Intema, H.T.; Mulcahy, D.D.; Röttgering, H.J.A.; van Weeren, R.J.; et al. Deep LOFAR observations of the merging galaxy cluster CIZA J2242.8+5301. *Mon. Not. R. Astron. Soc.* **2017**, *471*, 1107–1125. [[CrossRef](#)]
207. Kang, H.; Petrosian, V.; Ryu, D.; Jones, T.W. Injection of  $\kappa$ -like Suprathermal Particles into Diffusive Shock Acceleration. *Astrophys. J.* **2014**, *788*, 142. [[CrossRef](#)]
208. Zimbardo, G.; Perri, S. Understanding the radio spectral indices of galaxy cluster relics by superdiffusive shock acceleration. *Mon. Not. R. Astron. Soc.* **2018**, *478*, 4922–4930. [[CrossRef](#)]
209. Ge, C.; Liu, R.Y.; Sun, M.; Yu, H.; Rudnick, L.; Eilek, J.; Owen, F.; Dasadia, S.; Rossetti, M.; Markevitch, M.; et al. Chandra and XMM-Newton observations of A2256: Cold fronts, merger shocks, and constraint on the IC emission. *Mon. Not. R. Astron. Soc.* **2020**, *497*, 4704–4717. [[CrossRef](#)]
210. Churazov, E.; Khabibullin, I.; Bykov, A.M.; Lyskova, N.; Sunyaev, R. Tempestuous life beyond R500: X-ray view on the Coma cluster with SRG/eROSITA. II. Shock & Relic. *arXiv* **2022**, arXiv:2205.07511.
211. Wittor, D.; Etori, S.; Vazza, F.; Rajpurohit, K.; Hoeft, M.; Domínguez-Fernández, P. Exploring the spectral properties of radio relics—I: Integrated spectral index and Mach number. *Mon. Not. R. Astron. Soc.* **2021**, *506*, 396–414. [[CrossRef](#)]
212. Hoeft, M.; Nuza, S.E.; Gottlöber, S.; van Weeren, R.J.; Röttgering, H.J.A.; Brügggen, M. Radio Relics in Cosmological Simulations. *J. Astrophys. Astron.* **2011**, *32*, 509–517. [[CrossRef](#)]
213. Wittor, D.; Hoeft, M.; Vazza, F.; Brügggen, M.; Domínguez-Fernández, P. Polarization of radio relics in galaxy clusters. *Mon. Not. R. Astron. Soc.* **2019**, *490*, 3987–4006. [[CrossRef](#)]
214. Roh, S.; Ryu, D.; Kang, H.; Ha, S.; Jang, H. Turbulence Dynamo in the Stratified Medium of Galaxy Clusters. *Astrophys. J.* **2019**, *883*, 138. [[CrossRef](#)]
215. Russell, H.R.; Nulsen, P.E.J.; Caprioli, D.; Chadayammuri, U.; Fabian, A.C.; Kunz, M.W.; McNamara, B.R.; Sanders, J.S.; Richard-Laferrrière, A.; Beleznyay, M.; et al. The structure of cluster merger shocks: Turbulent width and the electron heating time-scale. *Mon. Not. R. Astron. Soc.* **2022**, *514*, 1477–1493. [[CrossRef](#)]

216. Domínguez-Fernández, P.; Brügggen, M.; Vazza, F.; Banda-Barragán, W.E.; Rajpurohit, K.; Mignone, A.; Mukherjee, D.; Vaidya, B. Morphology of radio relics—I. What causes the substructure of synchrotron emission? *Mon. Not. R. Astron. Soc.* **2020**, *500*, 795–816.
217. Bonafede, A.; Giovannini, G.; Feretti, L.; Govoni, F.; Murgia, M. Double relics in Abell 2345 and Abell 1240. Spectral index and polarization analysis. *Astron. Astrophys.* **2009**, *494*, 429–442. [[CrossRef](#)]
218. Kale, R.; Dwarakanath, K.S.; Bagchi, J.; Paul, S. Spectral and polarization study of the double relics in Abell 3376 using the Giant Metrewave Radio Telescope and the Very Large Array. *Mon. Not. R. Astron. Soc.* **2012**, *426*, 1204–1211. [[CrossRef](#)]
219. Stuardi, C.; Bonafede, A.; Rajpurohit, K.; Brügggen, M.; de Gasperin, F.; Hoang, D.; van Weeren, R.J.; Vazza, F. Using the polarization properties of double radio relics to probe the turbulent compression scenario. *Astron. Astrophys.* **2022**, *666*, A8. [[CrossRef](#)]
220. Laing, R.A. A model for the magnetic-field structure in extended radio sources. *Mon. Not. R. Astron. Soc.* **1980**, *193*, 439–449. [[CrossRef](#)]
221. Di Gennaro, G.; van Weeren, R.J.; Rudnick, L.; Hoeft, M.; Brügggen, M.; Ryu, D.; Röttgering, H.J.A.; Forman, W.; Stroe, A.; Shimwell, T.W.; et al. Downstream Depolarization in the Sausage Relic: A 1-4 GHz Very Large Array Study. *Astrophys. J.* **2021**, *911*, 3. [[CrossRef](#)]
222. Domínguez-Fernández, P.; Brügggen, M.; Vazza, F.; Hoeft, M.; Banda-Barragán, W.E.; Rajpurohit, K.; Wittor, D.; Mignone, A.; Mukherjee, D.; Vaidya, B. Morphology of radio relics—II. Properties of polarized emission. *Mon. Not. R. Astron. Soc.* **2021**, *507*, 2714–2734. [[CrossRef](#)]
223. Hoeft, M.; Rajpurohit, K.; Wittor, D.; di Gennaro, G.; Domínguez-Fernández, P. On the Polarisation of Radio Relics. *Galaxies* **2022**, *10*, 10. [[CrossRef](#)]
224. de Gasperin, F.; Brunetti, G.; Brügggen, M.; van Weeren, R.; Williams, W.L.; Botteon, A.; Cuciti, V.; Dijkema, T.J.; Edler, H.; Iacobelli, M.; et al. Reaching thermal noise at ultra-low radio frequencies. Toothbrush radio relic downstream of the shock front. *Astron. Astrophys.* **2020**, *642*, A85. [[CrossRef](#)]
225. Wittor, D. On the Challenges of Cosmic-Ray Proton Shock Acceleration in the Intracluster Medium. *New Astron.* **2021**, *85*, 101550. [[CrossRef](#)]
226. Blasi, P.; Colafrancesco, S. Cosmic rays, radio halos and nonthermal X-ray emission in clusters of galaxies. *Astropart. Phys.* **1999**, *12*, 169–183. [[CrossRef](#)]
227. Wiener, J.; Oh, S.P.; Guo, F. Cosmic ray streaming in clusters of galaxies. *Mon. Not. R. Astron. Soc.* **2013**, *434*, 2209–2228. [[CrossRef](#)]
228. Pinzke, A.; Oh, S.P.; Pfrommer, C. Turbulence and particle acceleration in giant radio haloes: The origin of seed electrons. *Mon. Not. R. Astron. Soc.* **2017**, *465*, 4800–4816. [[CrossRef](#)]
229. Ha, J.H.; Ryu, D.; Kang, H.; van Marle, A.J. Proton Acceleration in Weak Quasi-parallel Intracluster Shocks: Injection and Early Acceleration. *Astrophys. J.* **2018**, *864*, 105. [[CrossRef](#)]
230. Ha, J.H.; Ryu, D.; Kang, H. Gamma-ray and Neutrino Emissions due to Cosmic-Ray Protons Accelerated at Intracluster Shocks in Galaxy Clusters. *arXiv* **2019**, arXiv:1910.02429.
231. Ryu, D.; Kang, H.; Ha, J.H. A Diffusive Shock Acceleration Model for Protons in Weak Quasi-parallel Intracluster Shocks. *Astrophys. J.* **2019**, *883*, 60. [[CrossRef](#)]
232. Wittor, D.; Vazza, F.; Ryu, D.; Kang, H. Limiting the shock acceleration of cosmic ray protons in the ICM. *Mon. Not. R. Astron. Soc.* **2020**, *495*, L112–L117. [[CrossRef](#)]
233. Wittor, D.; Vazza, F.; Brügggen, M. Studying the Effect of Shock Obliquity on the  $\gamma$ -ray and Diffuse Radio Emission in Galaxy Clusters. *Galaxies* **2016**, *4*, 71. [[CrossRef](#)]
234. Wittor, D.; Vazza, F.; Brügggen, M. Testing cosmic ray acceleration with radio relics: A high-resolution study using MHD and tracers. *Mon. Not. R. Astron. Soc.* **2017**, *464*, 4448–4462. [[CrossRef](#)]
235. Banfi, S.; Vazza, F.; Wittor, D. Shock waves in the magnetized cosmic web: The role of obliquity and cosmic ray acceleration. *Mon. Not. R. Astron. Soc.* **2020**, *496*, 3648–3667. [[CrossRef](#)]
236. Giacintucci, S.; Markevitch, M.; Johnston-Hollitt, M.; Wik, D.R.; Wang, Q.H.S.; Clarke, T.E. Discovery of a Giant Radio Fossil in the Ophiuchus Galaxy Cluster. *Astrophys. J.* **2020**, *891*, 1. [[CrossRef](#)]
237. Gupta, N.; Huynh, M.; Norris, R.P.; Wang, X.R.; Hopkins, A.M.; Andernach, H.; Koribalski, B.S.; Galvin, T.J. Discovery of peculiar radio morphologies with ASKAP using unsupervised machine learning. *Publ. Astron. Soc. Aust.* **2022**, *39*, e051. [[CrossRef](#)]
238. Rahaman, M.; Raja, R.; Datta, A. On the detection of multiple shock fronts in A1914 using deep Chandra X-ray observations. *Mon. Not. R. Astron. Soc.* **2022**, *509*, 5821–5835. [[CrossRef](#)]
239. Mandal, S.; Intema, H.T.; van Weeren, R.J.; Shimwell, T.W.; Botteon, A.; Brunetti, G.; de Gasperin, F.; Brügggen, M.; Di Gennaro, G.; Kraft, R.; et al. Revived fossil plasma sources in galaxy clusters. *Astron. Astrophys.* **2020**, *634*, A4. [[CrossRef](#)]
240. de Gasperin, F.; Intema, H.T.; Shimwell, T.W.; Brunetti, G.; Brügggen, M.; Enßlin, T.A.; van Weeren, R.J.; Bonafede, A.; Röttgering, H.J.A. Gentle reenergization of electrons in merging galaxy clusters. *Sci. Adv.* **2017**, *3*, e1701634. [[CrossRef](#)]
241. Botteon, A.; Giacintucci, S.; Gastaldello, F.; Venturi, T.; Brunetti, G.; van Weeren, R.J.; Shimwell, T.W.; Rossetti, M.; Akamatsu, H.; Brügggen, M.; et al. Nonthermal phenomena in the center of Abell 1775. An 800 kpc head-tail, revived fossil plasma and slingshot radio halo. *Astron. Astrophys.* **2021**, *649*, A37. [[CrossRef](#)]

242. Pasini, T.; Edler, H.W.; Brügger, M.; de Gasperin, F.; Botteon, A.; Rajpurohit, K.; van Weeren, R.J.; Gastaldello, F.; Gaspari, M.; Brunetti, G.; et al. Particle re-acceleration and diffuse radio sources in the galaxy cluster Abell 1550. *Astron. Astrophys.* **2022**, *663*, A105. [[CrossRef](#)]
243. Giacintucci, S.; Venturi, T.; Markevitch, M.; Bourdin, H.; Mazzotta, P.; Merluzzi, P.; Dallacasa, D.; Bardelli, S.; Sikhosana, S.P.; Smirnov, O.; et al. A Candle in the Wind: A Radio Filament in the Core of the A3562 Galaxy Cluster. *Astrophys. J.* **2022**, *934*, 49. [[CrossRef](#)]
244. Hodgson, T.; Bartalucci, I.; Johnston-Hollitt, M.; McKinley, B.; Vazza, F.; Wittor, D. Ultra-steep-spectrum Radio “Jellyfish” Uncovered in A2877. *Astrophys. J.* **2021**, *909*, 198. [[CrossRef](#)]
245. Brienza, M.; Shimwell, T.W.; de Gasperin, F.; Bikmaev, I.; Bonafede, A.; Botteon, A.; Brügger, M.; Brunetti, G.; Burenin, R.; Capetti, A.; et al. A snapshot of the oldest active galactic nuclei feedback phases. *Nat. Astron.* **2021**, *5*, 1261–1267. [[CrossRef](#)]
246. Brienza, M.; Lovisari, L.; Rajpurohit, K.; Bonafede, A.; Gastaldello, F.; Murgia, M.; Vazza, F.; Bonnassieux, E.; Botteon, A.; Brunetti, G.; et al. The galaxy group NGC 507: Newly detected AGN remnant plasma transported by sloshing. *Astron. Astrophys.* **2022**, *661*, A92. [[CrossRef](#)]
247. Norris, R.P.; Crawford, E.; Macgregor, P. Odd Radio Circles and Their Environment. *Galaxies* **2021**, *9*, 83. [[CrossRef](#)]
248. Norris, R.P.; Collier, J.D.; Crocker, R.M.; Heywood, I.; Macgregor, P.; Rudnick, L.; Shabala, S.; Andernach, H.; da Cunha, E.; English, J.; et al. MeerKAT uncovers the physics of an odd radio circle. *Mon. Not. R. Astron. Soc.* **2022**, *513*, 1300–1316. [[CrossRef](#)]
249. Koribalski, B.S.; Norris, R.P.; Andernach, H.; Rudnick, L.; Shabala, S.; Filipović, M.; Lenc, E. Discovery of a new extragalactic circular radio source with ASKAP: ORC J0102-2450. *Mon. Not. R. Astron. Soc.* **2021**, *505*, L11–L15. [[CrossRef](#)]
250. Koribalski, B.S.; Veronica, A.; Brügger, M.; Reiprich, T.H.; Dolag, K.; Heywood, I.; Andernach, H.; Dettmar, R.J.; Hoeft, M.; Zhang, X.; et al. MeerKAT discovery of a double radio relic and odd radio circle. *arXiv* **2023**, arXiv:2304.11784. <https://doi.org/10.48550/arXiv.2304.11784>.
251. Omar, A. Odd radio circles as supernovae remnants in the intragroup medium. *Mon. Not. R. Astron. Soc.* **2022**, *513*, 101–105. [[CrossRef](#)]
252. Filipović, M.D.; Payne, J.L.; Alsaberi, R.Z.E.; Norris, R.P.; Macgregor, P.J.; Rudnick, L.; Koribalski, B.S.; Leahy, D.; Ducci, L.; Kothes, R.; et al. Mysterious odd radio circle near the large magellanic cloud—An intergalactic supernova remnant? *Mon. Not. R. Astron. Soc.* **2022**, *512*, 265–284. [[CrossRef](#)]
253. Sarbadhicary, S.K.; Thompson, T.A.; Lopez, L.A.; Mathur, S. On Odd Radio Circles as Supernova Remnants. *arXiv* **2022**, arXiv:2209.10554.
254. Kirillov, A.A.; Savelova, E.P. Possible formation of ring galaxies by torus-shaped magnetic wormholes. *Eur. Phys. J. C* **2020**, *80*, 810. [[CrossRef](#)]
255. Kirillov, A.A.; Savelova, E.P.; Vladykina, P.O. Possible Effects of the Fractal Distribution of Relic Wormholes. *Universe* **2021**, *7*, 178. [[CrossRef](#)]
256. Beck, A.M.; Dolag, K.; Lesch, H.; Kronberg, P.P. Strong magnetic fields and large rotation measures in protogalaxies from supernova seeding. *Mon. Not. R. Astron. Soc.* **2013**, *435*, 3575–3586. [[CrossRef](#)]
257. Botteon, A.; van Weeren, R.J.; Brunetti, G.; de Gasperin, F.; Intema, H.T.; Osinga, E.; Di Gennaro, G.; Shimwell, T.W.; Bonafede, A.; Brügger, M.; et al. A giant radio bridge connecting two galaxy clusters in Abell 1758. *Mon. Not. R. Astron. Soc.* **2020**, *499*, L11–L15. [[CrossRef](#)]
258. Bonafede, A.; Brunetti, G.; Vazza, F.; Simionescu, A.; Giovannini, G.; Bonnassieux, E.; Shimwell, T.W.; Brügger, M.; van Weeren, R.J.; Botteon, A.; et al. The Coma Cluster at Low Frequency ARray Frequencies. I. Insights into Particle Acceleration Mechanisms in the Radio Bridge. *Astrophys. J.* **2021**, *907*, 32. [[CrossRef](#)]
259. Brügger, M.; Reiprich, T.H.; Bulbul, E.; Koribalski, B.S.; Andernach, H.; Rudnick, L.; Hoang, D.N.; Wilber, A.G.; Duchesne, S.W.; Veronica, A.; et al. Radio observations of the merging galaxy cluster system Abell 3391-Abell 3395. *Astron. Astrophys.* **2021**, *647*, A3. [[CrossRef](#)]
260. Brunetti, G.; Vazza, F. Second-order Fermi Reacceleration Mechanisms and Large-Scale Synchrotron Radio Emission in Intracluster Bridges. *Phys. Rev. Lett.* **2020**, *124*, 051101. [[CrossRef](#)] [[PubMed](#)]
261. Jedamzik, K.; Pogossian, L. Relieving the Hubble Tension with Primordial Magnetic Fields. *Phys. Rev. Lett.* **2020**, *125*, 181302. [[CrossRef](#)]
262. Vacca, V.; Murgia, M.; Govoni, F.; Enßlin, T.; Oppermann, N.; Feretti, L.; Giovannini, G.; Loi, F. Magnetic Fields in Galaxy Clusters and in the Large-Scale Structure of the Universe. *Galaxies* **2018**, *6*, 142. [[CrossRef](#)]
263. Vazza, F.; Ferrari, C.; Bonafede, A.; Brügger, M.; Gheller, C.; Braun, R.; Brown, S. Filaments of the radio cosmic web: Opportunities and challenges for SKA. In Proceedings of the Advancing Astrophysics with the Square Kilometre Array (AASKA14), Giardini Naxos, Italy, 9–13 June 2014; p. 97.
264. Vernstrom, T.; West, J.; Vazza, F.; Wittor, D.; Riseley, C.J.; Heald, G. Polarized accretion shocks from the cosmic web. *Sci. Adv.* **2023**, *9*, eade7233. [[CrossRef](#)]
265. Neronov, A.; Vovk, I. Evidence for Strong Extragalactic Magnetic Fields from Fermi Observations of TeV Blazars. *Science* **2010**, *328*, 73. [[CrossRef](#)] [[PubMed](#)]
266. Braun, R.; Bourke, T.; Green, J.A.; Keane, E.; Wagg, J. Advancing Astrophysics with the Square Kilometre Array. In Proceedings of the Advancing Astrophysics with the Square Kilometre Array (AASKA14), Giardini Naxos, Italy, 9–13 June 2014; p. 174. [[CrossRef](#)]

267. Merloni, A.; Predehl, P.; Becker, W.; Böhringer, H.; Boller, T.; Brunner, H.; Brusa, M.; Dennerl, K.; Freyberg, M.; Friedrich, P.; et al. eROSITA Science Book: Mapping the Structure of the Energetic Universe. *arXiv* **2012**, arXiv:1209.3114.
268. ZuHone, J.A.; Markevitch, M.; Ruszkowski, M.; Lee, D. Cold Fronts and Gas Sloshing in Galaxy Clusters with Anisotropic Thermal Conduction. *Astrophys. J.* **2013**, *762*, 69. [[CrossRef](#)]
269. Lazarian, A.; Xu, S. Diffusion of Cosmic Rays in MHD Turbulence with Magnetic Mirrors. *Astrophys. J.* **2021**, *923*, 53. [[CrossRef](#)]
270. Montanino, D.; Vazza, F.; Mirizzi, A.; Viel, M. Enhancing the Spectral Hardening of Cosmic TeV Photons by Mixing with Axionlike Particles in the Magnetized Cosmic Web. *Phys. Rev. Lett.* **2017**, *119*, 101101. [[CrossRef](#)]
271. Basu, A.; Goswami, J.; Schwarz, D.J.; Urakawa, Y. Searching for Axionlike Particles under Strong Gravitational Lenses. *Phys. Rev. Lett.* **2021**, *126*, 191102. [[CrossRef](#)]
272. Berezhinsky, V.S.; Blasi, P.; Ptuskin, V.S. Clusters of Galaxies as Storage Room for Cosmic Rays. *Astrophys. J.* **1997**, *487*, 529–535. [[CrossRef](#)]
273. Hackstein, S.; Vazza, F.; Brüggen, M.; Sorce, J.G.; Gottlöber, S. Simulations of ultra-high energy cosmic rays in the local Universe and the origin of cosmic magnetic fields. *Mon. Not. R. Astron. Soc.* **2018**, *475*, 2519–2529. [[CrossRef](#)]
274. Dolag, K.; Bartelmann, M.; Lesch, H. SPH simulations of magnetic fields in galaxy clusters. *Astron. Astrophys.* **1999**, *348*, 351–363.
275. Shimwell, T.W.; Röttgering, H.J.A.; Best, P.N.; Williams, W.L.; Dijkema, T.J.; de Gasperin, F.; Hardcastle, M.J.; Heald, G.H.; Hoang, D.N.; Horneffer, A.; et al. The LOFAR Two-metre Sky Survey. I. Survey description and preliminary data release. *Astron. Astrophys.* **2017**, *598*, A104. [[CrossRef](#)]
276. Shimwell, T.W.; Hardcastle, M.J.; Tasse, C.; Best, P.N.; Röttgering, H.J.A.; Williams, W.L.; Botteon, A.; Drabent, A.; Mechev, A.; Shulevski, A.; et al. The LOFAR Two-metre Sky Survey. V. Second data release. *Astron. Astrophys.* **2022**, *659*, A1. [[CrossRef](#)]
277. McConnell, D.; Hale, C.L.; Lenc, E.; Banfield, J.K.; Heald, G.; Hotan, A.W.; Leung, J.K.; Moss, V.A.; Murphy, T.; O'Brien, A.; et al. The Rapid ASKAP Continuum Survey I: Design and first results. *Publ. Astron. Soc. Aust.* **2020**, *37*, e048. [[CrossRef](#)]
278. Hale, C.L.; McConnell, D.; Thomson, A.J.M.; Lenc, E.; Heald, G.H.; Hotan, A.W.; Leung, J.K.; Moss, V.A.; Murphy, T.; Pritchard, J.; et al. The Rapid ASKAP Continuum Survey Paper II: First Stokes I Source Catalogue Data Release. *Publ. Astron. Soc. Aust.* **2021**, *38*, e058. [[CrossRef](#)]
279. Knowles, K.; Cotton, W.D.; Rudnick, L.; Camilo, F.; Goedhart, S.; Deane, R.; Ramatsoku, M.; Bietenholz, M.F.; Brüggen, M.; Button, C.; et al. The MeerKAT Galaxy Cluster Legacy Survey. I. Survey Overview and Highlights. *Astron. Astrophys.* **2022**, *657*, A56. [[CrossRef](#)]
280. Gupta, Y.; Ajithkumar, B.; Kale, H.S.; Nayak, S.; Sabhapathy, S.; Sureshkumar, S.; Swami, R.V.; Chengalur, J.N.; Ghosh, S.K.; Ishwara-Chandra, C.H.; et al. The upgraded GMRT: Opening new windows on the radio Universe. *Curr. Sci.* **2017**, *113*, 707–714. [[CrossRef](#)]
281. Lal, D.V. Upgraded GMRT Observations of the Coma Cluster of Galaxies: The Observations. *Astrophys. J. Suppl. Ser.* **2020**, *250*, 22. [[CrossRef](#)]
282. Perley, R.A. The VLA Upgrade. In *American Astronomical Society Meeting Abstracts*; American Astronomical Society: Madison, WI, USA, 1996; Volume 188, p. 895.

**Disclaimer/Publisher's Note:** The statements, opinions and data contained in all publications are solely those of the individual author(s) and contributor(s) and not of MDPI and/or the editor(s). MDPI and/or the editor(s) disclaim responsibility for any injury to people or property resulting from any ideas, methods, instructions or products referred to in the content.